Seismic volcanostratigraphy of the western Indian rifted margin: The pre-Deccan igneous province

Gérôme Calvès,[1,2,3] Anne M. Schwab,[4] Mads Huuse,[5] Peter D. Clift,[1] Carmen Gaina,[6,7] David Jolley,[1] Ali R. Tabrez,[8] and Asif Inam[8]

Received 8 January 2010; revised 24 September 2010; accepted 13 October 2010; published 20 January 2011.

[1] The Indian Plate has been the focus of intensive research concerning the flood basalts of the Deccan Traps. Here we document a volcanostratigraphic analysis of the offshore segment of the western Indian volcanic large igneous province, between the shoreline and the first magnetic anomaly (An 28 ~63 Ma). We have mapped the different crustal domains of the NW Indian Ocean from stretched continental crust through to oceanic crust, using seismic reflection and potential field data. Two volcanic structures, the Somnath Ridge and the Saurashtra High, are identified, extending ~305 km NE–SW in length and 155 km NW–SE in width. These show the internal structures of buried shield volcanoes and hyaloclastic mounds, surrounded by mass-wasting deposits and volcanic sediments. The structures observed resemble seismic images from the North Atlantic and northwest Australia, as well as volcanic geometries described for Réunion and Hawaii. The geometry and internal seismic facies within the volcanic basement suggest a tholeiitic composition and subaerial to shallow marine emplacement. At the scale of the western Indian Plate, the emplacement of this volcanic platform is constrained by structural lineations associated with rifting. By reviewing the volcanism in the Indian Ocean and plate reconstruction of the area, the timing of the volcanism can be associated with eruption of a pre-Deccan continental flood basalt (~75–65.5 Ma). The volcanic platform in this study represents an addition of 19–26.5% to the known volume of the West Indian Volcanic Province.

Citation: Calvès, G., A. M. Schwab, M. Huuse, P. D. Clift, C. Gaina, D. Jolley, A. R. Tabrez, and A. Inam (2011), Seismic volcanostratigraphy of the western Indian rifted margin: The pre-Deccan igneous province, *J. Geophys. Res.*, *116*, B01101, doi:10.1029/2010JB000862.

1. Introduction

[2] Passive continental margin and the geometries of the continent-ocean transition have previously been studied using multidisciplinary data sets including detailed bathymetry and potential field data (gravity and magnetics) that allow crustal domains to be differentiated into continental crust or stretched transitional, and accreted oceanic crust [e.g., *White*, 1992]. As seismic imaging technology has evolved, detailed information has been derived regarding the deep and lateral structure of rifted margins. Two main types of passive margins are recognized on the basis of occurrence, or not, of voluminous, usually subaerial, volcanism. Volcanic margins are characterized by widespread effusive and/or intrusive material associated with the onset of continental breakup [*Coffin and Edholm*, 1993, 1994]. Recent work on offshore large igneous provinces (LIPs) using 2-D long offset or 3-D seismic reflection data has increased our understanding of the heterogeneity and spatial variation in volcanic terrains along passive volcanic margins [e.g., *Gernigon et al.*, 2004; *Thomson*, 2005, 2007; *Hansen*, 2006; *Hansen et al.*, 2008; *Rey et al.*, 2008]. These studies provide a new step in the way geoscientists observe and interpret rifting geometries and the formation of LIPs since the birth of seismic volcanostratigraphy compilation in the 1990s using 2-D seismic profiles and the framework outlined by *Planke et al.* [1999, 2000]. However, despite this new information, controversy continues concerning the source of the excess magmatism and whether it is linked to the presence of deep-seated mantle plumes, or whether it is a product of shallower lithospheric processes along these margins [e.g., *Lizarralde et al.*, 2007; *Calvès et al.*, 2008].

[3] Here we provide a detailed eruptive history of a well-developed rifted volcanic margin in the Arabian Sea in order

[1]Department of Geology and Petroleum Geology, School of Geosciences, University of Aberdeen, Aberdeen, UK.
[2]LMTG, CNRS, Toulouse, France.
[3]Now at LMTG, Université de Toulouse Paul Sabatier, SVT-OMP, Toulouse, France.
[4]Marathon International Petroleum (GB), Ltd., Aberdeen, UK.
[5]School of Earth, Atmospheric, and Environmental Sciences, University of Manchester, Manchester, UK.
[6]Geological Survey of Norway, Trondheim, Norway.
[7]PGP, Department of Geosciences, University of Oslo, Oslo, Norway.
[8]National Institute for Oceanography, Karachi, Pakistan.

0148-0227/11/2010JB000862

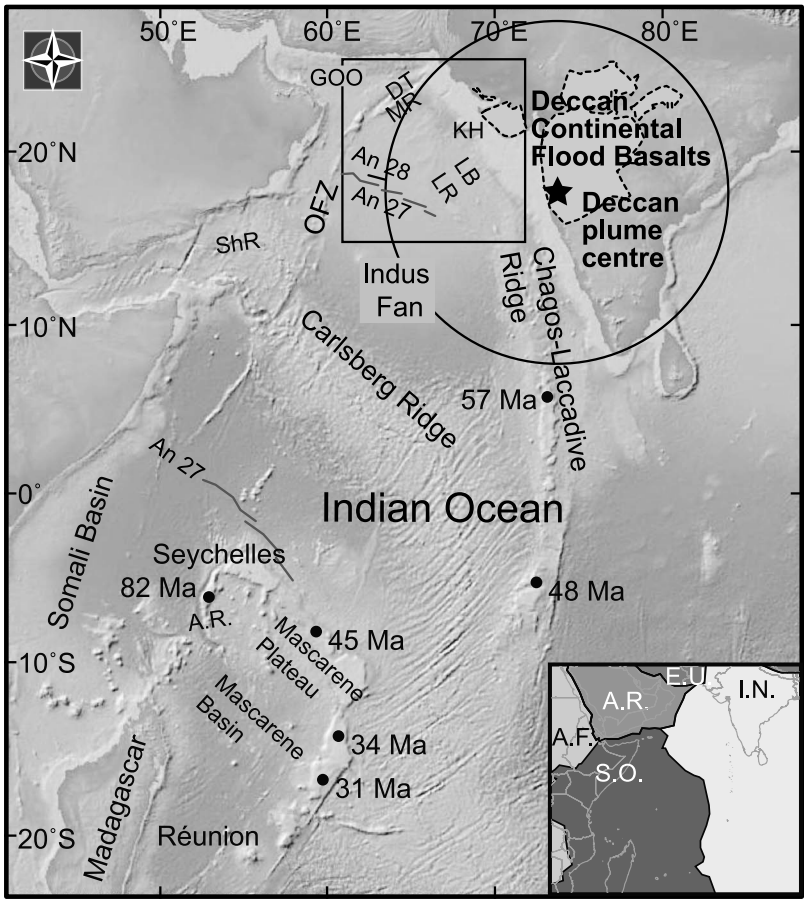

Figure 1. Location map with main morphologic features of the NE Arabian Sea. The black box is the study area covered by reflection seismic data. Major structural features are abbreviated as follows: MR, Murray Ridge; DT, Dalrymple Trough; OFZ, Owen Fault Zone; LR, Laxmi Ridge; LB, Laxmi Basin; GOO, Gulf of Oman; ShR, Sheiba Ridge; AR, Amirante Ridge. Black dots are ages of sampled basement (Amirante Ridge [*Fisher et al.*, 1968], Seychelles and Mascarene Plateau [*Duncan*, 1990], and Chagos-Laccadive [*Purdy and Bertram*, 1993]). Inset is a plate sketch of the area covered by Figure 1: E.U., Eurasia; I.N., Indian; A.R., Arabian; A.F., African; S.O., Somalian.

to understand the transition from a continental flood basalt province to the first seafloor spreading magnetic anomaly. In order to do this we (1) present an overview of published data and models for the western Indian rifted margin, (2) develop an integrated model of the offshore crustal structure using potential field data (gravity magnetics) coupled with subsurface seismic reflection data in order to generate a regional tectonic framework, (3) focus on a detailed study area using reflection seismic images to define the volcanostratigraphy of the margin, (4) place the evolution of the observed volcanic structures into a plate dynamic/rifting history, and finally (5) estimate the life span of the volcanism on the basis of calibrated production rates of volcanic activity.

2. Geological Framework

[4] The western rifted margin of the Indian Shield has received extensive attention concerning its tectonic history, as well as its impact on atmosphere–solid Earth–climate interactions. One of the most prominent and well-known features of the onshore geology is the Deccan Volcanic Province or Deccan Continental Flood Basalts, often referred to as the "Deccan Traps" (Figure 1). This province is one of the largest recognized LIPs (present cover of ~0.5 × 10^6 km^2) and is often interpreted to have been sources from the present day Réunion "hot spot" [*Mahoney*, 1988; *Duncan*, 1990]. The subsurface of the Great Deccan Province [*Todal and Edholm*, 1998] has not been imaged, as has been the case for other well known volcanic margins (e.g., Vøring, Rockall, Gascoyne). The breakup tectonics of this margin have been studied through the analysis of regional magnetic anomalies associated with the onset of seafloor spreading [*Bhattacharya et al.*, 1994; *Malod et al.*, 1997; *Royer et al.*, 2002]. However, only a few studies have sufficient subsurface imaging to allow detailed analysis of the deeper acoustic "basement" (i.e., below the sedimentary Cenozoic record of the Indus Fan, which covers the northwestern edge of the LIP offshore) [e.g., *Malod et al.*, 1997; *Gaedicke et al.*, 2002; *Collier et al.*, 2008]. To date, only a few seismic refraction profiles have attempted to

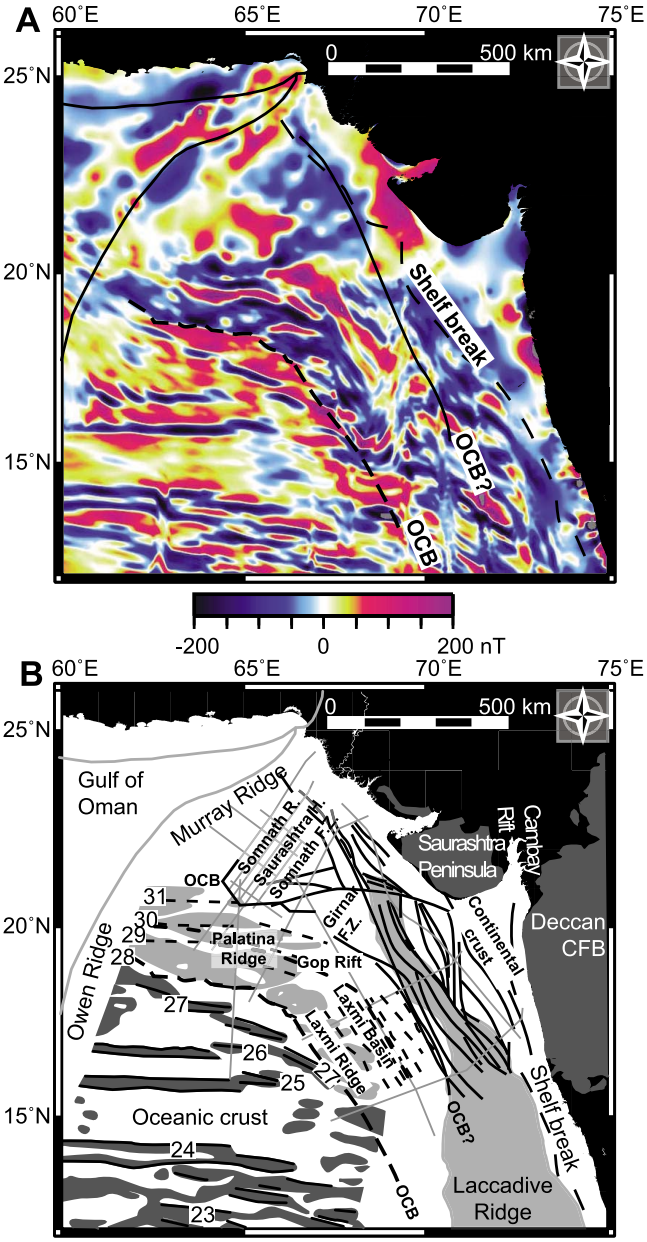

Figure 2. Magnetic maps of the study area. (a) Magnetic anomaly map compiled from EMAG2 model [*Maus et al.*, 2009]. (b) Published interpreted magnetic anomaly picks (An 25–31) (see references within text). The regional magnetic field structure can be divided into two main domains: one SW of the previously published Ocean Continent Boundary (OCB), where magnetic lineations along an E–W direction related to oceanic spreading are clearly imaged, and another NE of the OCB, where magnetic highs and lows constrain more localized rounded features and NW–SE elongated structures. CFB, continental flood basalt.

unravel the geometry of the margin [e.g., *Naini and Talwani*, 1982; *Minshull et al.*, 2008].

[5] The plate tectonic organization of the NW Indian Ocean reflects the multiphase breakup history between Africa, Madagascar, Seychelles and India associated with extensive magmatic activity, as well as the subsequent collision with Eurasia around 50 Ma [e.g., *Norton and Sclater*, 1979; *Gombos et al.*, 1995; *Lee and Lawver*, 1995]. The breakup of eastern Gondwanaland started at ~165 Ma or even earlier [*Eagles and König*, 2008; *König and Jokat*, 2010] between the Africa-Somalia plates, East Antarctica and the Madagascar-India-Australia blocks, followed by the breakup between greater India and Australia in Late Jurassic [*Heine et al.*, 2004] and between India and the Antarctica in the Cretaceous (~128 ± 2 Ma) [*Gaina et al.*, 2007]. Around 85–90 Ma Seychelles-India separated from Madagascar and created the Mascarene Basin [*Storey et al.*, 1995] (Figure 1). The subsequent opening of the Gop Rift (Figure 2b) was recently suggested to be dated to an early reversed polarity interval 31r (68.7–71.0 Ma), potentially associated with a pre-Deccan phase of magmatism [*Collier et al.*, 2008]. *Yatheesh et al.* [2009] recently challenged the age model of the Gop Rift/Basin by modeling magnetic anomalies and spreading rates and proposed two rift model the first between A31r-A25r (~69.3–56.4 Ma) and a second from A29r to A25r (~64.8–56.4 Ma).

[6] Finally the Seychelles-India block migrated north with the opening of the Laxmi Basin (Figures 1 and 2) starting ~67 Ma [e.g., *Bhattacharya et al.*, 1994; *Malod et al.*, 1997], which was followed by the eruption of the Deccan continental flood basalts ~65 Ma and separation of India from the Seychelles [e.g., *Bernard and Munschy*, 2000; *Courtillot et al.*, 2000; *Collier et al.*, 2008, and references within].

3. Data and Methods

[7] Study of the present day rifted margin structure can be pursued by integrating subsurface imaging (seismic reflection data) and potential field data (i.e., gravity and magnetics) at regional scales, together with modeling to refine and test crustal geometries at local scales. We use this approach with a set of potential field data from the public domain and exploration seismic reflection images released to us for research purposes. The deep imaging of margins has traditionally been carried out by acquisition of seismic refraction profiles, but modern seismic reflection with long streamer acquisition is leading the petroleum industry now that hydrocarbon exploration is targeting deeper objectives (up to 18 s two-way time). Only a limited number of such deep refraction profiles exist in the area of interest [*Naini and Talwani*, 1982; *Minshull et al.*, 2008].

3.1. Potential Field Data

[8] The gravity data we analyze here are from the compilation v16.1 of *Sandwell and Smith* [1997]. The magnetic regional model used in this study is from the EMAG2 model [*Maus et al.*, 2009] (Figure 2a). Associated with this magnetic model, magnetic anomaly picks in the oceanic domain are from *Bhattacharya et al.* [1994], *Malod et al.* [1997], *Royer et al.* [2002], *Chaubey et al.* [1998, 2002], and *Todal and Edholm* [1998] (Figure 2b).

[9] In order to define the crustal structure of the margin, potential field data such as gravity or magnetics can be used as primary information. Processing and filtering methods allow vertical or wavelength variation of crustal bodies to be extracted [*Gernigon et al.*, 2004; *Rey et al.*, 2008; *Pawlowski*, 2008; *Antobreh et al.*, 2009; *Barrère et al.*, 2009]. Compilation of regional anomalies and projection

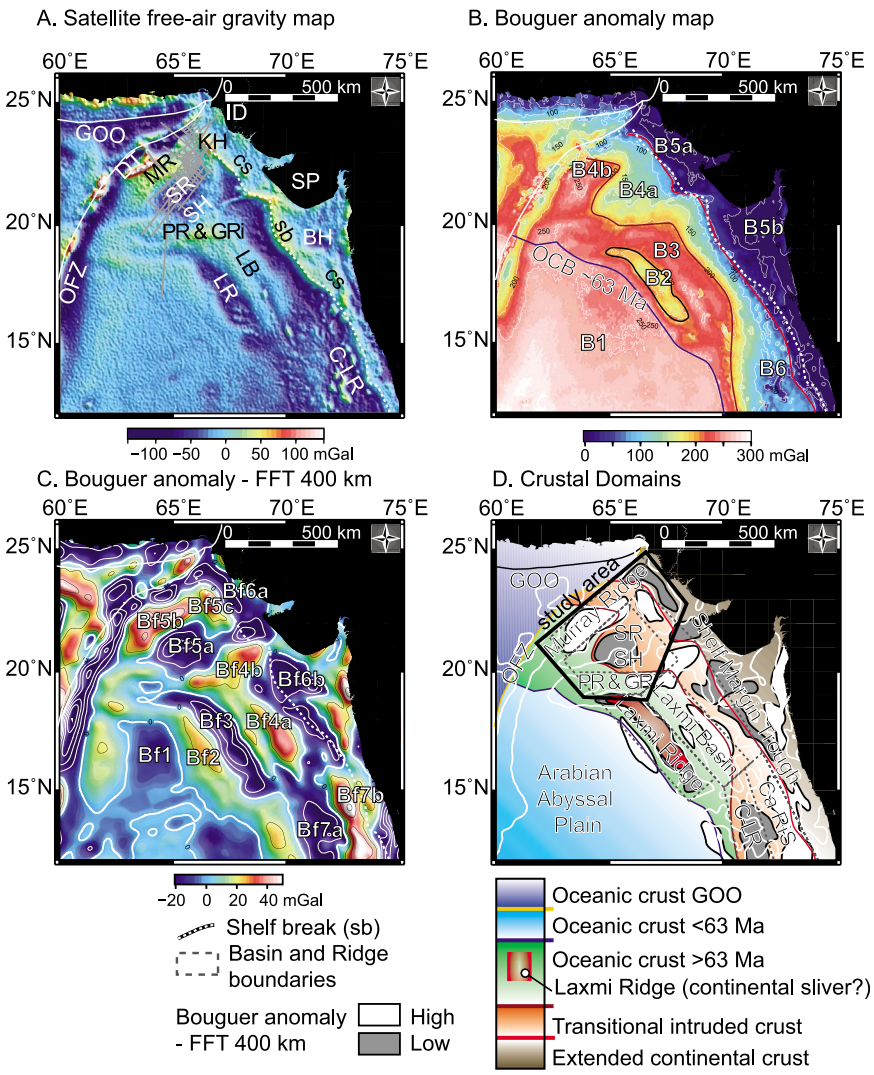

Figure 3. Gravity maps of the study area. (a) Satellite free-air gravity map (abbreviated structural features are same as those in Figure 1). SH, Saurashtra High; SR, Somnath Ridge; KH, Kori High; SP, Saurashtra Peninsula; BH, Bombay High; PR, Palatina Ridge; GRi, Gop Rift; cs, continental shelf. (b) Bouguer anomaly map (slab density 2670 kg/m^3) (numbers denote gravity anomalies explained in the text). This potential field map highlights the first-order crustal domains from continental to oceanic crust and the transitional crust. (c) The 400 km high pass filtered Bouguer gravity anomaly map (numbers denote gravity anomalies explained in the text). (d) Crustal domain compilation map, where high and low from Bouguer anomaly filtered (see Figure 3c) are outlined in white and grey, respectively. White contours represent 0 mGal of the 200 km high pass filtered Bouguer gravity anomaly map. Bold black line shows study area. Ca.Ri.S., Cannanore Rift System.

of data along strike from the seismic lines allows the crustal domains and transition zones along this rifted continental margin to be interpreted (Figure 3d).

[10] A slab density of 2670 kg/m^3 (typical crustal density) was used on the satellite gravity free-air anomaly, in association with bathymetric data [*Intergovernmental Oceanographic Commission*, 2003] in order to compute the Bouguer gravity field (Figure 3b). The Bouguer anomaly identifies "anomalous masses," that is, masses with density above or below the slab density used [*Blakely*, 1995]. Filters in the frequency domain (fast Fourier transforms) were applied, which are equivalent to 400 km (Figure 3c) and 200 km, high pass on the Bouguer data in order to derive information on regional variations at Moho and basement depth within the study area.

3.2. Seismic Reflection Data

[11] One of the most challenging aspects of the seismic reflection method applied to volcaniclastic rocks is the discontinuity and high lateral-vertical variation of this particular geological medium. A good seismic reflection image can only be obtained with suitable acquisition and processing parameters, in particular by picking enough coherently stacked common midpoints (CMP) below the "seismic basement" surface. A compilation of different seismic reflection surveys has been used for this study (Table 1).

Table 1. Seismic Survey Data Used in This Study and Previous Published Works Using These Data for Various Research Aspects[a]

Survey Name	Acquisition	Type	Number of Seismic Lines/Total Length (km)	Source Type/Volume (cubic inches)	Cable Length (m)/ Coverage (Fold)	Vertical Record (Second Two-Way Time)	Frequency Content (Hz) (Range/Dominant)	Published Works
PAK 77	Conoco Phillips	2-D poststack migrated	9/1083	Air gun array/1705 (reprocessed by Shell E&P in 2000)	2750/NA	8	5–70/10–40	*Deptuck et al.* [2003]
SO-122	BGR	2-D poststack migrated	9/1550	NA	600–3000/variable	10	5–80/20–50	*Gaedicke et al.* [2002]
PAK 99	Shell	2-D poststack migrated	30/2200	Air gun array/1500	5087.5/102	8	5–70/25–50	*Deptuck et al.* [2003]
TEPP 00	TOTAL	2-D poststack migrated	23/4210	Air gun array/3410	5000/80	10–12	5–90/15–50	*Calvès et al.* [2008]
CD 144	NOCS-NERC	2-D poststack migrated	3/700	Air gun array/3890	2400/48	12	12.5–50/20–35	*Collier et al.* [2008]

[a]NA, not available.

The majority of the seismic images displayed in this paper are from a seismic reflection data set obtained with 6 km long streamers and a long record time (10 to >12 s two-way travel time (TWT)). As an example of the relative high quantity of the stacking velocity picks used below the top seismic basement we plot the root mean square (RMS) stacking velocity along one seismic reflection line (Figure 4a). This density of stacking velocity picks allows the recognition of continuous events below the seismic basement and the observation of geometrical features.

[12] The overall bandwidth of the 2-D seismic reflection profiles is 5–90 Hz (Figure 4b, light grey continuous curves). The bandwidth below the regional basement surface-volcaniclastic facies (under the Indus Fan Megasequence [*Droz and Bellaiche*, 1991]) is 5–60 Hz, with a peak frequency content of about 20 Hz (Figure 4b, black dots). For a basement of "volcanic" or "volcaniclastic" composition, with velocities ranging from ~3.5–4.5 km/s in the upper layers and up to >6.0 km/s in the lower layers, the vertical resolution below basement (defined as a quarter of the wavelength) ranges from 22 to 100 m (equivalent to: 3.5 km/s – 40 Hz; 6.0 km/s –15 Hz).

[13] We have extracted velocity information from the stacking velocities using a geological layered model approach. This information is plotted in a velocity-depth profile (Figure 4c) and is compared to "classic" reference velocity profiles from different rifted margins or oceanic plateaus. A compilation of three different crustal velocity profile groups are plotted for reference: a classic North Atlantic volcanic rifted margin [*Hopper et al.*, 2003; *Spence et al.*, 1989], local profiles in the Gop Rift to Laxmi Ridge south of the study area [*Minshull et al.*, 2008] and finally oceanic plateaus such as Ontong-Java, Kerguelen and Agulhas [*Gohl and Uenzelmann-Neben*, 2001, and references within].

[14] Most of the velocity profiles observed in our study area have a closer affinity with oceanic plateaus rather than "classic" profiles of rifted margins, such as the North Atlantic or even south of the study area in the Gop Rift and Laxmi Basin (Figure 4c). We observe that even if the stacking velocities tend to lower the "true" velocity by 5–10% during seismic processing, this information is still relevant for estimating interval velocities in the reflections below the top seismic basement. Furthermore, experience from the Vøring margin offshore Norway and equivalent volcanic margin terrains indicates that wide-angle refraction experiments tend to overestimate interval velocities by >0.4 km/s in the upper section of the extruded crust, at least compared to values derived from vertical seismic profiles, those measured for physical properties or calculated from stacking velocities [*Planke and Eldholm*, 1994].

[15] In our study area no boreholes have yet penetrated the basement. On the southern portion of the Saurashtra volcanic platform (Indian exclusive economic zone; Figure 2b) two exploration boreholes penetrated ~50 m of the Cretaceous basaltic "basement" (http://www.dghindia.org; wells: GSDW2A-1 and GSDW1-1).

3.3. Seismic Volcanostratigraphy

[16] The seismic volcanostratigraphic concept employed here is inherited from *Mitchum et al.* [1977] and is based on seismic stratigraphy and sequence stratigraphy methods

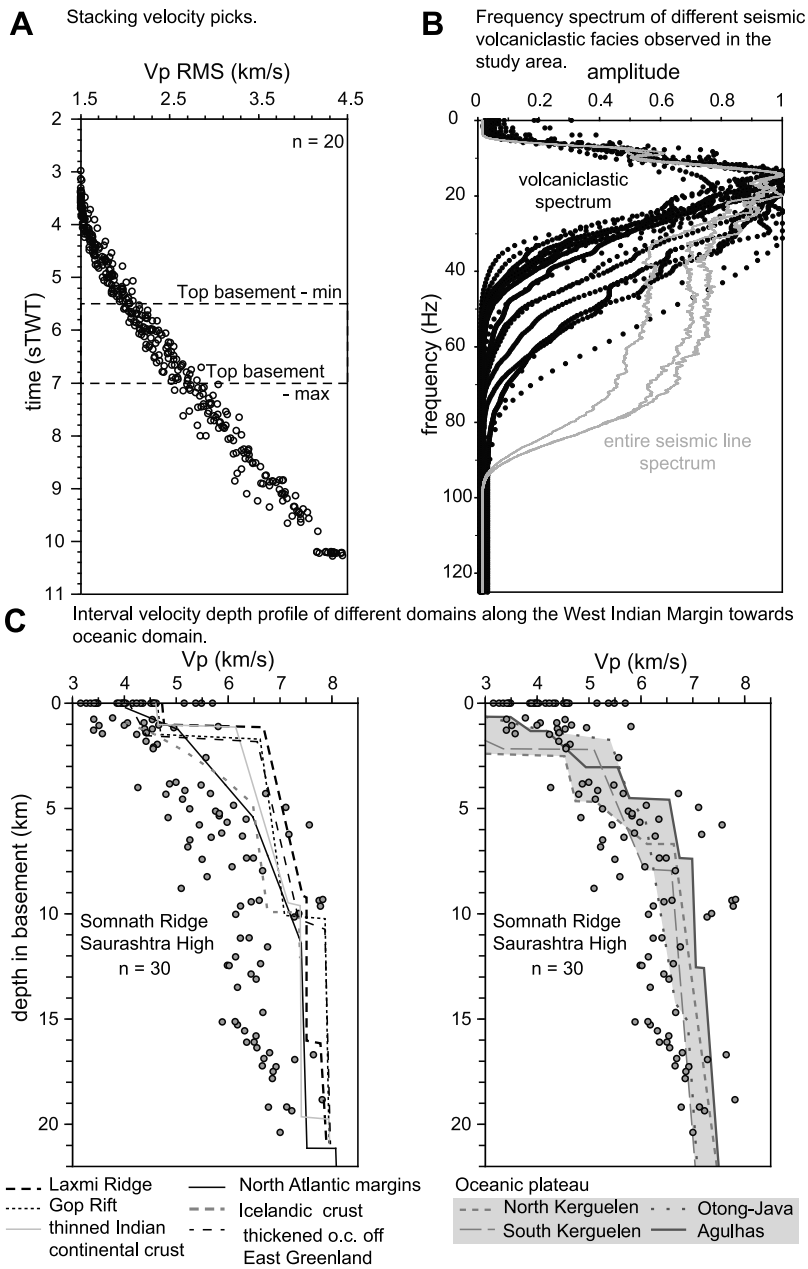

Figure 4. Velocity plots from study area. (a) Velocity-time plot of the RMS stacking velocity used along one line in the seismic reflection processing flow. (b) Frequency content of the seismic reflection data below top volcaniclastic basement (black dots) and entire spectrum of three seismic lines (grey curves). (c) Velocity crustal profiles of Laxmi Basin, Laxmi Ridge, oceanic domain with recent velocities [*Minshull et al.*, 2008] along the Gop Rift, and edge of Saurashtra High; grey dots are interval velocity extracted along the Somnath Ridge and Saurashtra High from seismic stacking velocities in the study area (30 pseudowells; same points on both plots). Reference curves for Atlantic volcanic margins are plotted for reference in the left plot [*White*, 1992; *Hopper et al.*, 2003]. Oceanic plateau velocity profiles from Kerguelen, Otong Java, and Agulhas [*Gohl and Uenzelmann-Neben*, 2001] are plotted for reference in the right plot. This analysis of velocity profiles highlights the potential of volcanic origin crust within the study area, similar to other major oceanic plateaus in the Indian Ocean.

developed in the early 1970s on siliciclastic and carbonate sedimentary systems. This method was then applied to the observation and recognition of volcanic or volcaniclastic sedimentary systems along rifted volcanic margins [*Symonds et al.*, 1998; *Kiørboe*, 1999; *Planke et al.*, 1999, 2000]. Firstly, the seismic volcanostratigraphy interpretation leads to the identification of a basaltic sequence. Secondly, identification and interpretation of characteristic internal sequence reflections leads to the definition of volcanic seismic facies units and edifices. Finally, the seismic

facies observations are then interpreted in terms of volcanic and sedimentary processes, as shown in previous studies [*Symonds et al.*, 1998; *Planke et al.*, 1999, 2000; *Berndt et al.*, 2001; *Rey et al.*, 2008]. The mapping of the seismic facies and reflection stacking patterns differs from the classic scheme of clastic seismic sequence stratigraphy. Concepts such as the nonunique lateral transition of facies, are hard to apply with sparse seismic reflection grids and limited predictive seismic facies correlation calibrated with equivalent active volcanic depositional systems. This will be highlighted in the following sections.

4. Observations and Results

4.1. Potential Field Maps

4.1.1. Magnetic Field Data and Picks

[17] The oldest magnetic anomalies (An 28 ~ 63 Ma to An 27 ~ 61 Ma) that are related to the onset of seafloor spreading along the Carlsberg Ridge have been the subject of significant earlier studies (Figures 1 and 2b) [e.g., *Royer et al.*, 2002]. Magnetic anomalies related to earlier seafloor spreading in the Laxmi Basin and Gop Rift (see *Bhattacharya et al.* [1994], *Malod et al.* [1997], *Miles et al.* [1998], and others) have been described and discussed (An 29 to 32n.2n) (Figure 2b). The pre-Deccan tectonic setting following the opening of the Mascarene Basin at ~83 Ma (An 34) to ~65 Ma (An 29) is still debated [*Gnos et al.*, 1997; *Molnar et al.*, 1988; *Miles et al.*, 1998; *Royer et al.*, 2002]. The EMAG2 model is used as a reference for the regional magnetic field (Figure 2a) [*Maus et al.*, 2009]. We use that study as a reference because we are mostly interested in defining the portion of the margin that has no clear magnetic spreading anomalies (Figure 2b). It has been noted that the continent-ocean boundary defined using global anomaly maps does not allow this domain boundary to be recognized as a specific magnetic event from satellite-derived measurements [*Hemant and Maus*, 2005].

[18] The link between the opening of the Mascarene Basin and the Laxmi Basin (Figure 1) remains unresolved [*Miles et al.*, 1998; *Bernard and Munschy*, 2000]. The rates of spreading and "jumps" in the axis of seafloor spreading within the two basins following the breakup of India-Seychelles and Madagascar at about 90 Ma is not yet resolved in plate models (discussed below). In particular, the effect of the "Deccan" event at ~65 Ma on the offshore portion of the rifted margin between the present day continental shelf and identified spreading anomalies <63 Ma remains unknown. This has been partially solved by recent wide-angle seismic experiments and magnetic anomaly modeling in the area, which integrates the conjugate margins of India and the Seychelles. The results include identification of the Gop Rift and lower crustal bodies under the Laxmi Ridge and the continental rise (equivalent to the Saurashtra High in this study) [*Minshull et al.*, 2008; *Collier et al.*, 2008]. Nevertheless, the internal structure of the upper crust is poorly documented. Here we synthesize all the data and plot major faults, compiled magnetic picks, and published ocean-continent boundaries (OCB) (Figure 2b).

4.1.2. Gravity Field Data and Filters

[19] Satellite free-air gravity data allow us to recognize the major morphotectonic domains in the Arabian Sea (Figure 3a). A prominent SW–NE gravity low marks the plate boundary between the Indian and Arabia plates, expressed by the Owen Fracture Zone and the Dalrymple Trough-Murray Ridge system (Figure 3a). The Murray Ridge trends NE–SW along the northwestern edge of the Indian Plate and is characterized by a high gravity signature. To the south a gravity low corresponds to the Somnath Ridge and the Saurashtra High, which has a NE–SW trending long axis. Toward the continental shelf and the Indus Delta, a gravity high is recorded at the shelf break transition known as the Kori High. South of 20°N and the onshore Saurashtra Peninsula (NW part of the Deccan Traps), the continental shelf shows a concentric gravity low corresponding to the Bombay High. In the oceanic domain, a NW–SE trending gravity low demarks the slope of the margin, followed along the same trend by the gravity depression of the Laxmi Basin and the Laxmi Ridge further seaward. This domain is separated at ~20°N by the gravity high known as the Gop Rift, which has an E–W trend. Further south of ~15°N a rough low gravity signature is assigned to the Chagos-Laccadive Ridge marking the migration axis of the Indian Plate to the north along the "Réunion" hotspot [*Duncan*, 1990].

[20] The signature of the simple Bouguer gravity field (crustal density of 2670 kg/m^3) allows recognition of a large anomaly B1 >250 mGal, corresponding to the oceanic crustal domain SW of the Laxmi Ridge, anomaly B2 (Figure 3b). Northeast of the Laxmi Ridge anomaly B3 is developed at the 200 mGal level, with values reaching 250 mGal within the oceanic crust of domain B1. This is likely related to the fact that the Laxmi Basin (Domain B3 in Figure 3b) is formed by an aborted rift and associated oceanic crust [*Henry et al.*, 2008]. North of these domains, a prominent low-level bulge (Domain B4a in Figure 3b) marks the Somnath Ridge and Saurashtra High, which are of volcanic origin (100–250 mGal). Domain B4b corresponds to the SW portion of the Murray Ridge, with gravity values equivalent to the oceanic domains >200 mGal. East of the shelf break (dashed curve in Figure 3b) gravity values decrease to 50–100 mGal within two domains (B5a and B5b) corresponding to the Indus shelf wedge and the Bombay High structure, respectively. To the southeast, Domain B6, lying between 150 and 0 mGal, shows small circular/elongated features that are related to the Chagos-Laccadive Ridge and correspond to the thickened crust linked to the migration of the Indian Plate over the Réunion "hotspot" track [e.g., *Henstock and Thompson*, 2004].

[21] The 400 km filtered Bouguer anomaly map allows recognition of deeper structures along the continental margin (Figure 3c). In the abyssal plain a gravity low (Bf1) trends NW–SE (Figure 3c). The transition to the gravity low of the Laxmi Ridge (Bf3) is marked by a prominent high (Bf2). East of the Laxmi Ridge a NW–SE gravity high (Bf4a) marks the Laxmi Basin. At the northern tip of the Laxmi Basin, a NE–SW gravity high (Bf4b) characterizes the Gop Rift and Palatina Ridge with a transition to a gravity low (Bf5a) with a NE–SW orientation equivalent to the bulk of the Somnath Ridge and Saurashtra High. Gravity high Bf5b to the north corresponds to the Murray Ridge, whereas anomaly Bf5c is related to the main depocenter located off the continental shelf and shelf edge. Along the NW–SE

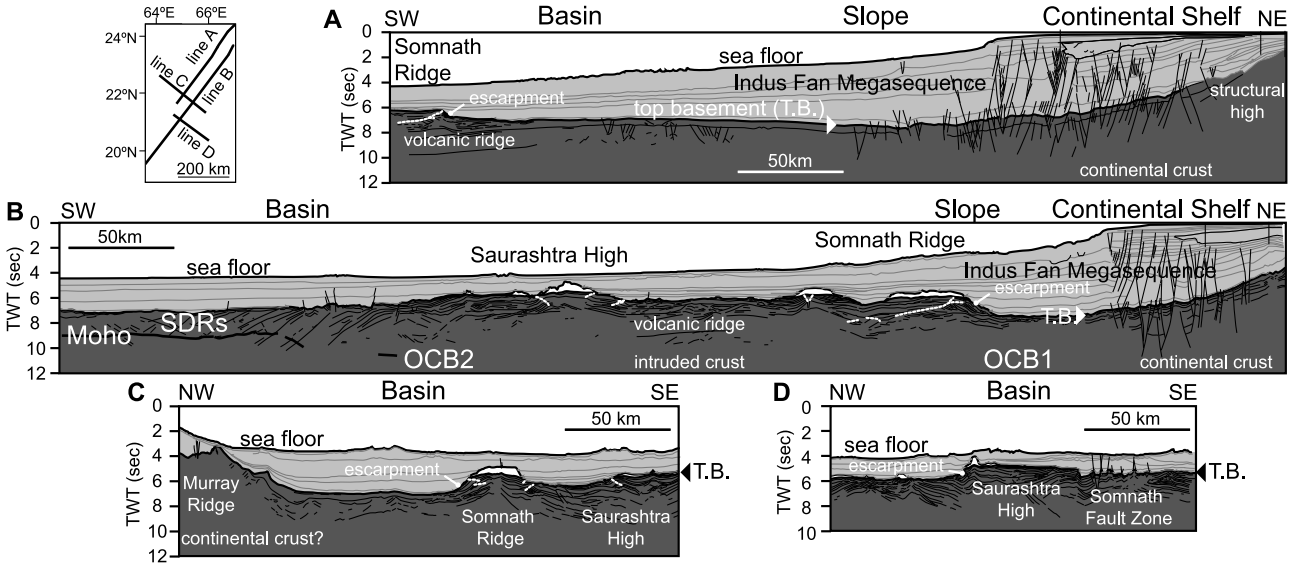

Figure 5. (a–d) Line drawings of four deep seismic lines illustrating the main geological features in the study area (location map in small inset, and line locations in Figure 6a). Top basement (T.B.) is the reflection at the top of the dark color, marking the regional occurrence of a high amplitude and continuous seismic reflection associated with the top of the Saurashtra High, Somnath Ridge, and the base of the Indus Fan Megasequence of Cenozoic age. This event marks the boundary between the rift to synrift deposits and the postrift sequence and is mapped in Figure 6b.

continental shelf (dashed white curve in Figure 3c), two gravity lows (Bf6a and Bf6b) are related to the Kori High and the Bombay High structure (Figure 3c).

[22] An intermediate filter of 200 km wavelength was used to produce another Bouguer anomaly map to bring out details of lateral variations between basement topography and the Indus Fan sedimentary sequence. In Figure 3d, the contours (white curve) displayed correspond to 0 mGal of the 200 km filter. We synthesize the crustal domains of the area in the following section using all the different gravity data.

4.2. Crustal Domains

[23] Crustal domains on volcanic margins may be difficult to define because the added magmatic material will modify the shape of the basement, the internal structure of the crust and the depth to Moho. Therefore, interpretation of structural trends and delineation of domains is open to discussion and spatial variation. On the western Indian rifted margin, at least two major rifting events are recorded. The first was associated with the separation of the Indian and Madagascar blocks (mid-Cretaceous) and the Seychelles and Indian blocks (Late Cretaceous). The second stage is associated with the aborted extension of the Laxmi Basin and the Gop Rift (Late Cretaceous–Paleocene) [e.g., *Naini and Talwani*, 1982; *Henry et al.*, 2008; *Minshull et al.*, 2008; *Collier et al.*, 2008]. Here we compile seismic images (stratigraphic and structural elements) and potential field data to define crustal domains from extended continental, transitional and oceanic crust (Figure 3d).

4.2.1. Extended Continental Crust

[24] Onshore the western rifted margin of India is mostly composed of the Deccan flood basalts (Figures 1 and 2b). The offshore portion from the shelf edge to the distal part of the margin toward the SW shows no clear high throw faults or rotated fault block geometries within the basement (Figures 5a and 5b), such as seen in West African or Iberia-type rifted margins. The main reason for this observed geometry is that blocks or high throw faults are not clearly seismically imaged beneath the basalt sequences related to the Deccan Trap volcanic rocks. In the NE Atlantic volcanic margins, fault blocks are observed but they are generally smaller and fewer compared to nonvolcanic rifted margins [*Larsen et al.*, 1994]. Nevertheless, along two regional profiles ~130 to 210 km of faulted basement, underlying the Indus Fan Megasequence, is observed below the continental shelf and the start of the slope (Figures 5a and 5b). This crust represents a domain of stretched continental crust related to the first breakup stage between Madagascar and India (Figures 2b and 3d, brown). Recent wide-angle seismic experiments suggest the presence of a block of extended continental crust between the Dalrymple Trough and Murray Ridge (NW of the study area in the Gulf of Oman, Figures 1 and 3a) [*Edwards et al.*, 2008]. However, we do not favor this interpretation because this lies seaward of our extended continental crust. Instead we propose that transitional intruded crust is more likely to be in the oceanic crust domain dated at >63 Ma (Figures 2b and 3d, orange).

4.2.2. Transitional Crust

[25] Intruded transitional crust or highly extended continental crust exists along the Western Indian Margin [e.g., *Malod et al.*, 1997; *Miles et al.*, 1998; *Gaedicke et al.*, 2002; *Clift et al.*, 2002; *Calvès et al.*, 2008]. The remaining question is the maximum extent of the extended continental crust along this margin. Some authors prefer to extend the ocean continent boundary – OCB (Figures 2a and 2b; OCB2 in Figure 5b) and the continental crust out to the first occurrence of the seaward dipping reflector sequences (SDRs) [*Malod et al.*, 1997; *Miles et al.*, 1998; *Gaedicke*

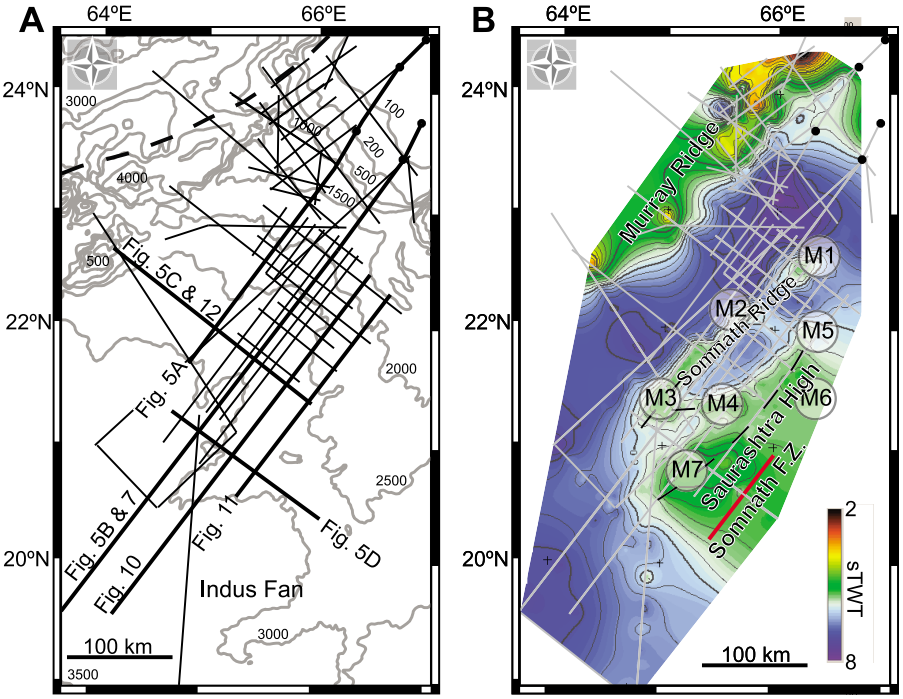

Figure 6. Seismic basement structure map. (a) Seabed depth contours (meters) and seismic data grid with figure locations. The seismic data within this paper are from survey TEPP00 (see Appendix A for acquisition survey parameters). (b) Regional seismic basement reflection time structure map (top of volcanic synrift sequence on the margin). Mound-shaped volcanic features are denoted by M1–M7. Note the scale of the Somnath Ridge and Saurashtra High, covering hundreds of kilometers.

et al., 2002], while others would extend the oceanic crust landward to near the modern shelf break [*Clift et al.*, 2002; *Calvès et al.*, 2008] (OCB? in Figures 2a and 2b; OCB1 in Figure 5b). The study area is itself characterized by the bulk of the Somnath Ridge and Saurashtra High, which are volcanic buildups located between the faulted continental crust and observed SDRs, that is, probable oceanic crust (Figures 3d and 5b). Subsidence and flexural analysis shows that the Somnath Ridge behaves like oceanic crust in this respect [*Calvès et al.*, 2008]. In this section, the use of transitional is chosen to define the domains of crustal affinity located around the ridge (to the SW of the ridge the first spreading anomaly marks the "true" oceanic crust, and to the NE of the volcanic platform the continental crust is part of the Indian continent). Therefore the Somnath Ridge and Saurashtra High are in a domain of transitional crust (either ultrastretched continental crust or old oceanic crust overprinted by volcanics).

[26] The most prominent feature along the western Indian rifted margin is the Chagos-Laccadive Ridge, which is generally interpreted as the product of the migration the Indian Plate over the Réunion "hot spot" between 65 Ma and ~48 Ma (Figure 1) [*Duncan*, 1990; *Purdy and Bertram*, 1993]. This ridge corresponds to intruded transitional crust (Figure 3d).

4.2.3. Oceanic Crust

[27] Oceanic crust is observed seaward of the Somnath Ridge and Saurashtra High as far as north of the spreading anomaly A28 (~63 Ma) (Figure 2b) and is characterized by voluminous SDRs, with a clear, underlying Moho reflection (Figure 5b). The thickness of this crust in the study area is estimated to be between 7.0 and 9.5 km (interval velocities ~6.8 km/s). This is in the range of oceanic crust and typical SDRs observed on equivalent volcanic margins along the U.S. East Coast or South Atlantic [*Oh et al.*, 1995; *Gladczenko et al.*, 1997, 1998]. A recent refraction profile is located SW of the study area and estimates crustal thickness along the same order of 7 to <10 km [*Minshull et al.*, 2008]. Oceanic crust may be present in the Laxmi Basin because some workers consider this basin to be an aborted rift with oceanic affinity [*Naini and Talwani*, 1982; *Bhattacharya et al.*, 1994; *Malod et al.*, 1997; *Henry et al.*, 2008; *Minshull et al.*, 2008]. On the neighboring plate NW of the Owen Fracture Zone in the Gulf of Oman, the crust is oceanic, and is estimated to be Jurassic–Early Cretaceous or Paleocene–Eocene, depending on the favored plate tectonic reconstruction (Figure 3d) [*White and Louden*, 1982; *Edwards et al.*, 2000, 2008].

4.3. Regional Basement Structure

[28] A regional seismic horizon is recognized on the seismic reflection profiles below the Indus Fan Megasequence that onlaps and infills the margin (TB on Figure 5) [*Droz and Bellaiche*, 1991]. This horizon corresponds to a high-amplitude reflection that is continuous and of regional lateral extent (Figure 5). On the basis of a 2-D seismic reflection data grid (Figure 6a) we have mapped this "seismic basement" surface, which lies at a depth between 2 and 8 s TWT (Figure 6b).

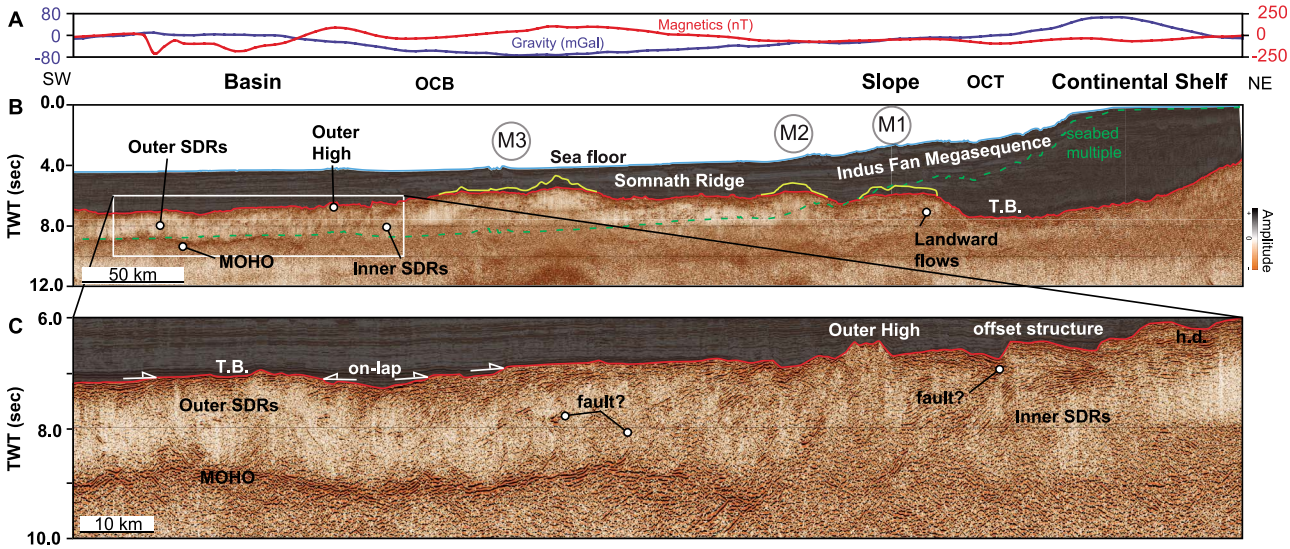

Figure 7. Seismic reflection line (orientation NE–SW). (a) Potential field data, (b) seismic image interpretation of Somnath Ridge and Saurashtra High (yellow curves are carbonates platforms overlying the seismic basement), and (c) detailed interpretation of white box in Figure 7b: seaward dipping reflector sequences (SDRs), Moho reflection, and hyaloclastic delta (h.d). This seismic line illustrates the typical geometry of the proximal (landward flows) to distal (SDRs) features observed on other volcanic margins. Line location is shown in Figure 6.

[29] Two deep linear trends characterize the present day basement geometry of the margin, running NE–SW and NW–SE (Figure 6b). The morphology of the basement structure is shown using a set of 2-D strike and dip seismic reflection profiles (Figure 6a), starting from the most seaward portion of the margin and as far landward as the continental shelf (Figures 5a and 5b). The regional structure of the basement in the study area (20–24°N, 64–67°E) is composed of three "structural highs." To the NW lies the Murray Ridge (Figures 5c and 6b), to the NE the basement shallows toward the continental shelf (Figures 5a, 5b, and 6b), and to the S lies the volcanic platform composed of the Saurashtra High and the Somnath Ridge (Figures 5 and 6b). Along a dip margin profile, a clear image of the SDRs and Moho reflection is recognized SW of the Saurashtra High (Figures 5b and 7). The gravity field value is mostly nil and gently turns to negative values toward the edge of the Outer High and the Inner SDRs, before the Saurashtra High which has strong negative gravity field values (Figures 3a and 7a). The morphology of the top basement reflection allows us to delineate three basement zones: the Outer SDRs (smooth top basement), an Outer High (local high at top basement) and the Inner SDRs (offset structure at top basement) (Figures 7b and 7c). To the northeast on the edge of the continental shelf-slope transition, the basement geometry is expressed by a prominent escarpment corresponding to the classic landward flows observed on other volcanic margins (Figure 7b) [*Planke et al.*, 1999, 2000]. Between the observed SDRs and this escarpment the basement structural high corresponds to the SW–NE oriented Somnath Ridge. The two NW–SE oriented profiles show a cross section across Somnath Ridge and Saurashtra High (Figures 5c and 5d). An extensive offshore carbonate platform is observed overlying each high volcanic ridge (yellow curves in Figure 7b) [*Calvès et al.*, 2008]. Previously, these deposits were inferred to be "prerift strata" of Cretaceous age [*Malod et al.*, 1997; *Gaedicke et al.*, 2002], but recent drilling results show a Paleogene age as their main growth stage, with final drowning in Miocene times [*Calvès*, 2009]. Southeast of the distal portion of the Saurashtra High we confirm the observation of *Malod et al.* [1997] of a faulted area known as the Somnath Fault Zone (Figures 5d and 6b). It is important to note that no major faults are observed on the top basement reflection of the volcanic ridge, except in the Inner SDRs and on the Murray Ridge (Figure 5).

[30] The area covered by the Somnath Ridge and Saurashtra High in the study area is ~42,500 km^2. This is a minimum estimation of the volcanic platform because the main part of the volcanic platform extends further to the southeast into the Indian offshore area, where we have little data. The morphology of the volcanic platform shows seven mounded structures labeled M1 to M7 (Figure 6b). Mounds 1 to 3 delineate the Somnath Ridge, M4 bridges this ridge to the Saurashtra High, which is composed of three mounds M5–M7 (Figure 6b). Morphometric measurements of each of these mounded structures are summarized in Table 2.

4.4. Volcanic Seismic Facies and Sequence Analysis

[31] The volcaniclastic features observed on reflection seismic data in the study area are shown in Figure 8, and named using adaptations to the schemes of *Symonds et al.* [1998] and *Planke et al.* [1999, 2000]. We use the schematic framework of *Symonds et al.* [1998] (Figure 9a) in addition to other seismic facies and edifices observed on volcanic margins or oceanic volcanic islands (Figure 9b). Inherited from the scheme of *Symonds et al.* [1998] and *Planke et al.* [1999, 2000], a landward flow corresponds to the progradation of a sequence of lava flows and/or hyaloclastic deltas toward the "land" (the Indian continent in this case), as opposed to the seaward direction where the

Table 2. Morphometric Measurement of Mounded Structures at Top Basement Reflection[a]

Mound	Seabed Depth TWT (s)	Seabed Depth Kilometers	Top Basement, TWT(s)	Length (km)	Width (km)	Area (10^3 km^2)
1	2.26	1.69	5.4	65.5	37.8	1.912
2	3.61	2.71	5.7	52.25	28	1.370
3	3.96	2.97	5.15	128	52	4.991
4	3.69	2.77	4.95	50.5	20.5	0.918
5	3.07	2.30	5.45	39	35	1.064
6	3.30	2.47	5.2	91	73	5.635
7	3.52	2.64	4.64	116.5	62	5.391

[a]Refer to Figure 6b for mound locations.

spreading and accretion of oceanic crust occurs. Morphometric measurements and seismic interval velocities are synthesized for each seismic volcanic feature in Figure 8.

[32] The main seismic volcanostratigraphic features observed below the top seismic basement horizon in the study area are as follows: SDRs (Outer and Inner), an Outer High, hyaloclastite deltas, lava flows, sill and saucer-shaped intrusions (Figure 8). These features combine to form the following types of volcanic edifices: shield volcanoes, hyaloclastic mounds and landward flows (Figure 8). The volcanic edifices are often laterally associated with mass-wasting and volcanic-derived sediments (Figure 8).

[33] The Outer and Inner SDRs, and the Outer High (Figures 7 and 9) have been previously discussed in the oceanic crust section. These features are limited to the southwest corner of the study area. A frequent observation along seismic profiles crossing the Somnath Ridge or the Saurashtra High is lava or hyaloclastite deltas (Figure 8 and Figures 9–12) [*Calvès et al.*, 2008]. In the study area, over 80 hyaloclastite deltas are identified on 2-D seismic images with characteristic topset and foreset geometries (Figures 9 and 10). The most rarely observed igneous seismic feature in the study area are saucer-shaped sills (Figure 8 and Figure 10c), which are extensively observed on other volcanic margins, either in the volcanic sequence or intruding the subsequent sedimentary basins [e.g., *Wood et al.*, 1988; *Joppen and White*, 1990].

[34] Figure 7 is a dip profile through the study area volcanic on the west Indian rifted margin. The distance between the landward flows and SDRs is ~300 km. In contrast, on classic volcanic rifted margins (North or South Atlantic type) distances between these features range from only ~50 km to a maximum of 100 km [e.g., *Eldholm and Grue*, 1994]. We now compare observations from these classic volcanic rifted margins to the internal organization of the volcanic edifices and ridges observed in the offshore Pakistan area.

[35] The largest edifices observed in the study area occur in the distal portion of the Saurashtra High and are bidirectional wedge-shaped edifices measuring 50 km wide and up to 2.2 s TWT (equivalent to >5 km) thick (M6 and M7 in Figures 9, 10, and 11b and Shield Volcano of Figure 8). The internal seismic reflection organization of these edifices are: parallel to subparallel topsets with low angles of inclination [*Emery and Myers*, 1996], chaotic reflections in the center of the edifice and foreset reflections at the edge corresponding to progradational hyaloclastite deltas (Figures 9c and 10c) [*Kiørboe*, 1999]. The gravity or magnetic field data do not show simple correlation to the size or center of the edifices. Along the Saurashtra High two edifices of this type are recognized (M6 and M7 in Figure 11b). The geometries of this type of edifice correspond to those seen in present day subaerial shield volcanoes, or those buried on volcanic margins. A small numbers of shield volcanoes have previously been documented on other volcanic margins [*Boldreel and Andersen*, 1994; *Gatliff et al.*, 1984], but are better known in other settings, such as Hawaii [*Walker*, 1990, 1993]. Some features recognized as seamounts in the NE Atlantic-Rockall region (e.g., Darwin, Sigmundur, and Rosemary Banks [*Archer et al.*, 2005]) could be considered as shield volcanoes or hyaloclastic mounds, but remain imperfectly documented.

[36] We define a hyaloclastic mound as a composite edifice made of spatially stacked hyaloclastic deltas, which is different from the definition of *Vail et al.* [1977] for the seismic geometry of a volcanic mound (Figure 13 and Figure 8). Two eruptive phases are distinguished in the build up of hyaloclastites in aqueous environments (lakes or oceans) [e.g., *Komatsu et al.*, 2004]. The first stage, or submerged eruption, shows an initial submarine extrusion of volcanic materials with a subhorizontal stratal geometry formed by tephra layers and/or pillow lavas. We refer to this stage of edifice construction as a pioneering cone (PC in Figures 13a and 13b). The second stage starts when edifice growth reaches sea level when the edifice shows subaerial eruptions that are characterized by topset and lava-fed deltas around the edges (Figures 13a and 13b). Morphometric measurement of these features allows a distinction to be made between the three major edifice types: hyaloclastic mounds (HM), landward flows (LF) and shield volcanoes (SV) (Figures 13b–13d). Hyaloclastic mounds show topset lengths from 2 to ~20 km, whereas landward flows and shield volcanoes are observed over distances of 24 to ~40 km (Figure 14d).

[37] Toward the NE of the Saurashtra High the more proximal shield volcano (M6) grades into landward flow geometries with complex stacked hyaloclastite and lava deltas (Figures 9b, 9d, and 10b). Further NE, the landward flow geometry is transient into a package lying below the top basement reflection, which is characterized by parallel reflections (Figures 9d and 10b). This seismic facies can be correlated to the base of the prograding lava deltas. This seismic facies is inferred to be made of volcanic sediments deposited below sea level.

[38] To the NW of the Somnath Ridge edifice, a trough of ~100 km width is expressed by a gravity high and a magnetic low (Figure 12a), which occurs before reaching the tilted and faulted Murray Ridge (Figure 12b). Below the top basement reflection a package of chaotic reflections under-

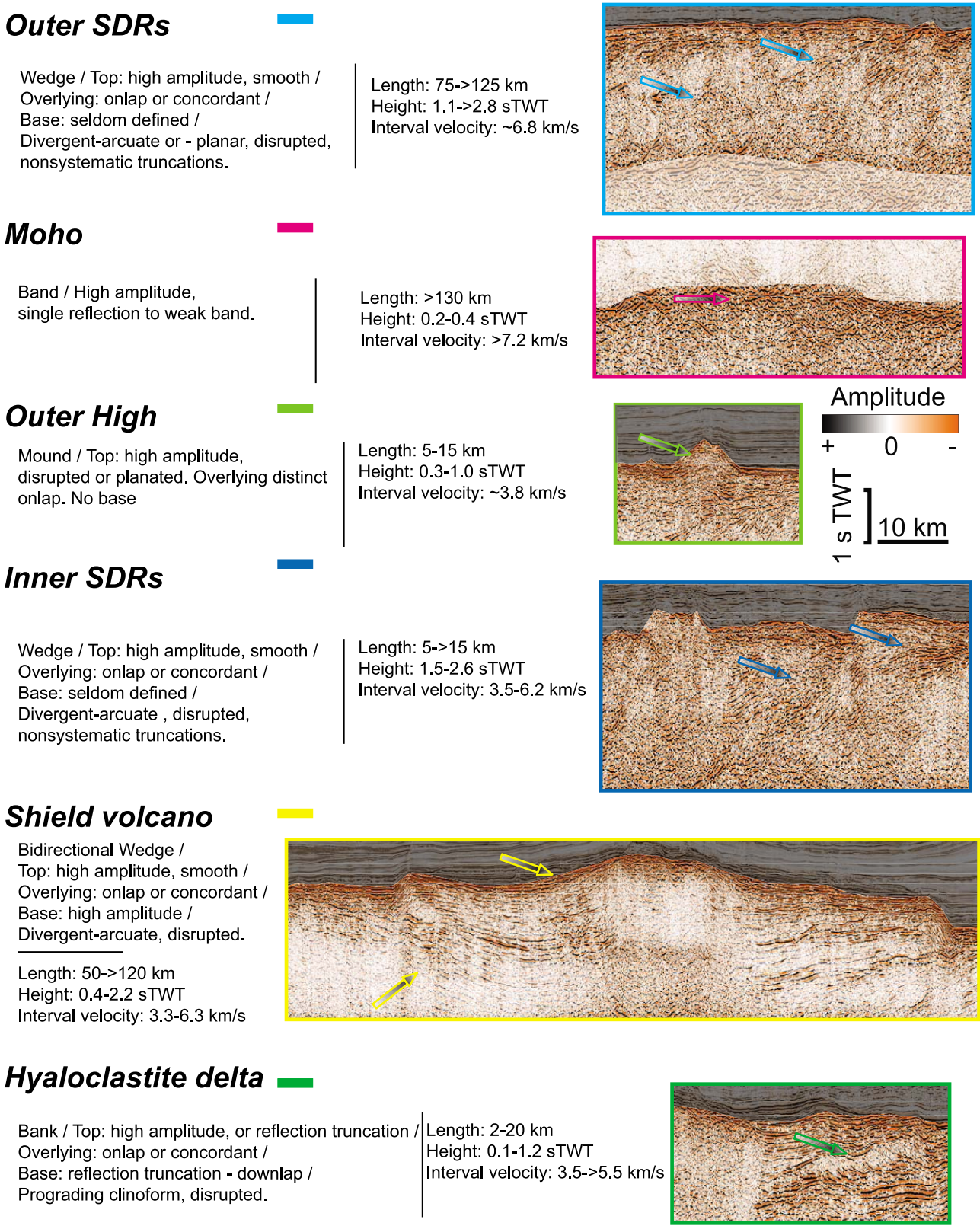

Figure 8. Seismic facies chart, morphometric data, and interpretation of the volcanostratigraphic elements of the study area (terminology adapted from *Planke et al.* [1999, 2000], *Rey et al.* [2008], and *Elliott and Parson* [2008]).

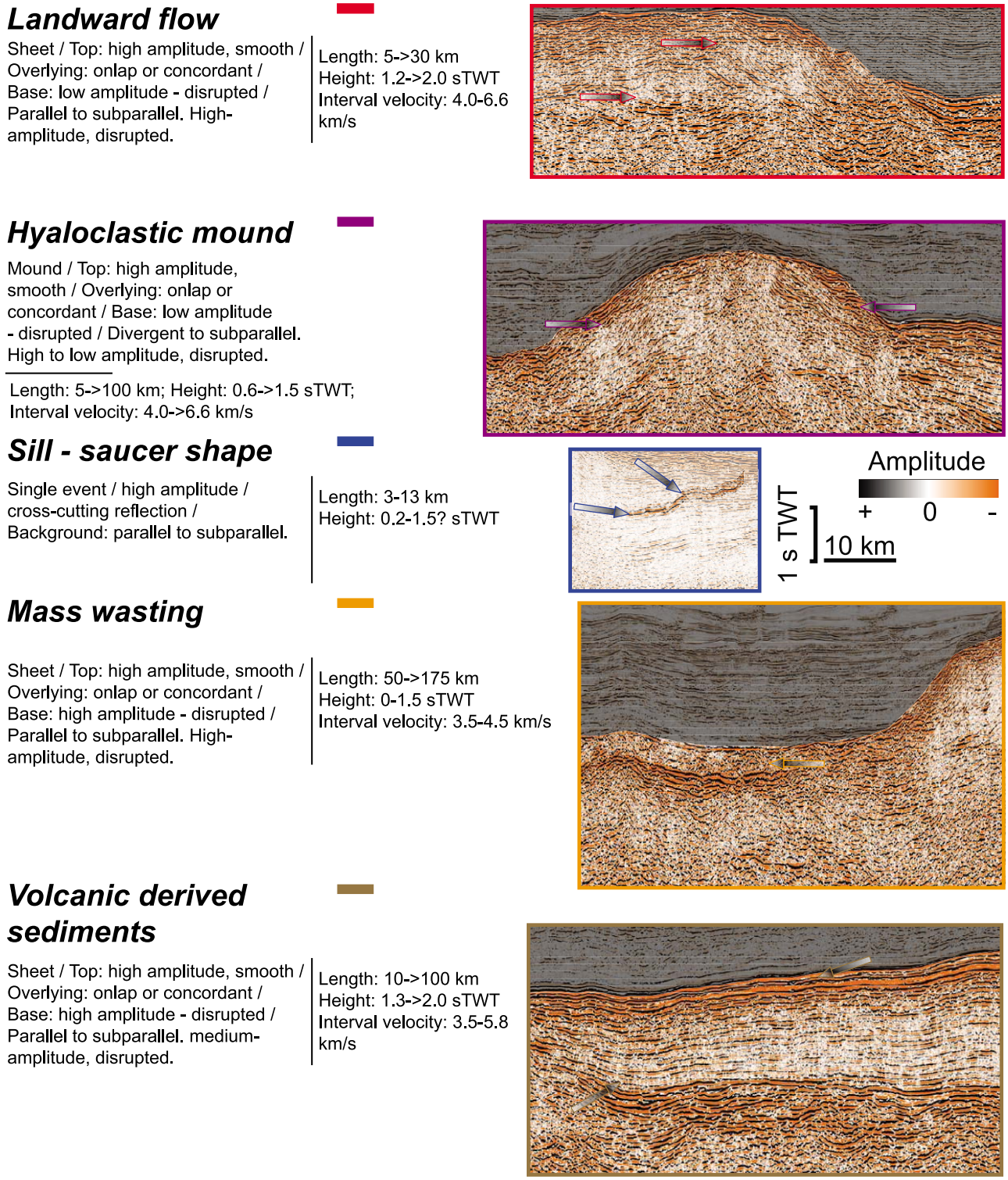

Figure 8. (continued)

lain by strong amplitude continuous reflections is observed (Figure 12b). This interval "pinches out" against a proto-Murray Ridge (Figures 6b and 11c), predating the generally accepted uplift of the present-day Murray Ridge at 20 Ma [*Mountain and Prell*, 1990] (Figure 12c). This package is interdigitated with the base of the foreset of the hyaloclastite deltas that form the Somnath Ridge escarpment (Figures 11b and 11d). On the NE side of Somnath Ridge the same

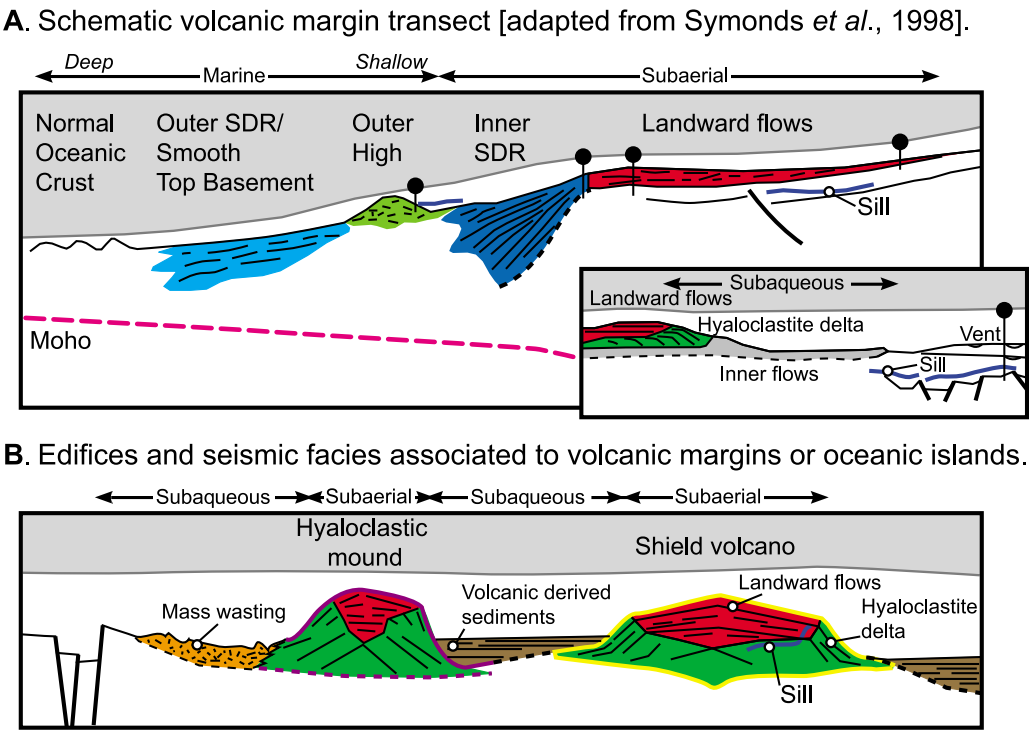

Figure 9. Volcanic margin framework, where the color of each element (outline) and facies is associated with the color scheme in Figure 8. (a) Schematic volcanic margin transect illustrating seismic facies units associated with extrusive volcanic deposits. Proposed emplacement environment (arrows) and wells (dots and lines) are schematically located (adapted from *Symonds et al.* [1998]), with SDRs. The inset in Figure 9a highlights the different elements within the landward flow sequence, using the nomenclature of *Symonds et al.* [1998]. (b) Schematic of other types of volcanic edifices and facies observed in volcanic margins or oceanic islands, synthesis from this study and analogy to volcanic edifices; see text for details.

seismic facies is observed. We associate these features with potential mass-wasting products from the volcanic ridge, and with erosion of the summit of the ridge or flank collapse from the edifices. This interpretation is based on a similarity with images from recent oceanic volcanic provinces. Mass wasting or landslides are well documented around present day oceanic volcanic provinces as imaged by detailed sea floor bathymetry or seismic reflection data or boreholes

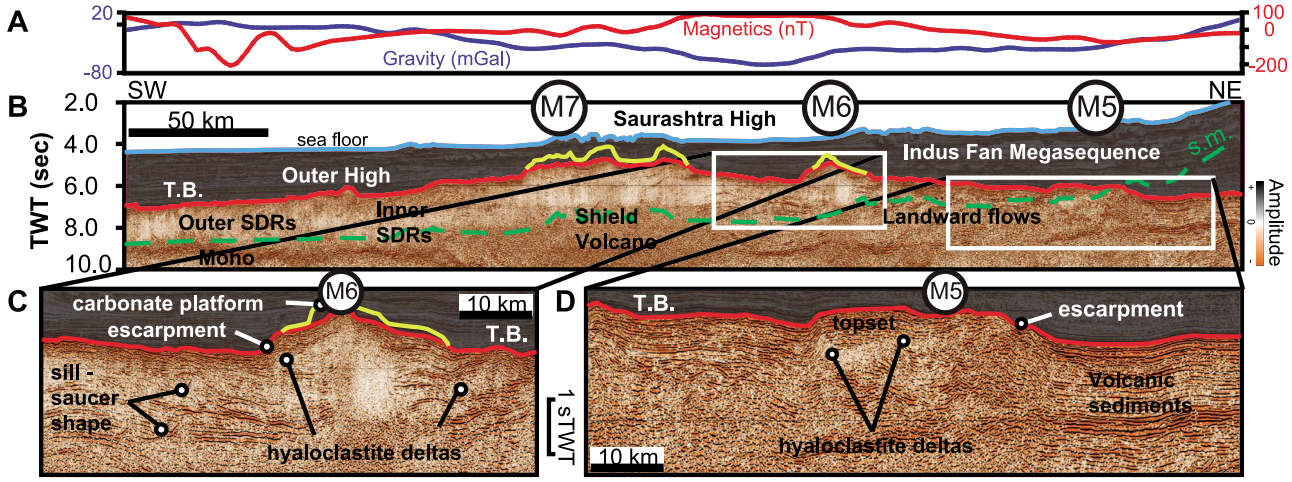

Figure 10. Seismic reflection line (orientation NE–SW). (a) Potential field data, (b) seismic image interpretation of Saurashtra High (green curve is seabed multiple), (c) sill saucer shape, hyaloclastite deltas, shield volcano geometry (note that the saucer-shape sills intrude the volcanic mound M6), and (d) hyaloclastic mound, topset lavas, and Saurashtra High NE escarpment to volcanic-derived sediments transition. Line location is shown in Figure 6.

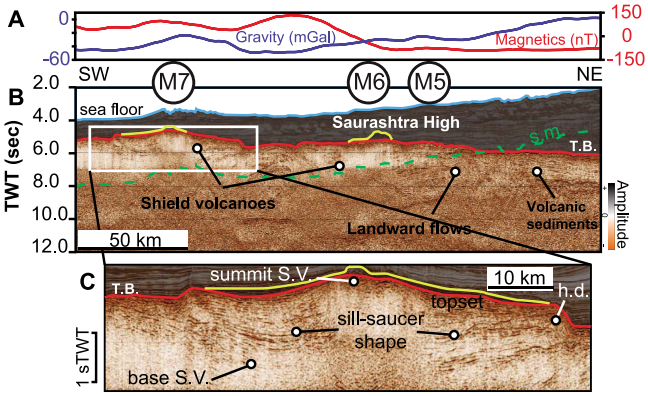

Figure 11. Seismic reflection line (orientation NE–SW). (a) Potential field data, (b) seismic image interpretation of Saurashtra High with interpretation of landward flows and volcanic-derived sediments (green curve is seabed multiple), and (c) interpretation of shield volcano (S.V.), with hyaloclastite deltas (h.d.). Note that the saucer-shape sill intrudes the shield volcano M7. Line location is shown in Figure 6.

(e.g., Hawaii [*Moore et al.*, 1989, 1994; *Presley et al.*, 1997], Canary Islands [*Funck and Schmincke*, 1998], Réunion [*de Voogd et al.*, 1999], and Cape Verde [*Masson et al.*, 2008]).

[39] Saucer-shaped sills intrude the volcaniclastic sequence, and are observed between the shield volcanoes M6 and M7 within the volcanic sediments (Figures 9c and 15a), as well as within these two shield volcanoes (Figures 10c and 15a). These features have also been observed in the NE Atlantic [*Larsen et al.*, 1994] where no feeder dykes are imaged on the seismic.

4.5. Volcanic Feature Mapping

[40] Using the seismic facies and geometries observed along the seismic grid we have mapped the major structural elements inside the Somnath Ridge and Saurashtra High, as well as in the surrounding areas (Figures 15 and 16a). The mounds recognized on the top basement structure (Figure 6b) can be identified as specific volcanic edifices: M1 through M5 are hyaloclastic mounds of elongated-rounded geometry, while M6 and M7 correspond to rounded, large shield-type volcanoes with a gentle top slope (Figures 15 and 16a). To the NE of the study area, a portion of the volcanic edifice corresponds to volcanic sediments (brown in Figure 16a). Between the Somnath Ridge (M1-4) and the Saurashtra High (M5-7) a NE–SW trending trough is infilled by subaqueous volcanic sediments. Mass-wasting products occur along the NW edge of the Somnath Ridge extending out toward the Murray Ridge (orange in Figure 16a). Some small cones are identified on the NW edge of the Somnath Ridge escarpment, whereas on the Saurashtra High cones are located in the cores of the shield volcanoes M6-M7, or on hyaloclastic mound M5 (orange dots in Figure 16a). Interestingly the observation of intrusive features such as sills and saucer-shaped intrusions is restricted to the shield volcanoes (M6, M7) and the region between these two edifices (blue lines in Figure 16a). Finally the seaward portion of the ridge may be related to the onset of seafloor spreading, characterized by extensive SDRs deposits (Figure 16a). The filtered 200 km Bouguer anomaly map images the different volcanic features and domains mapped

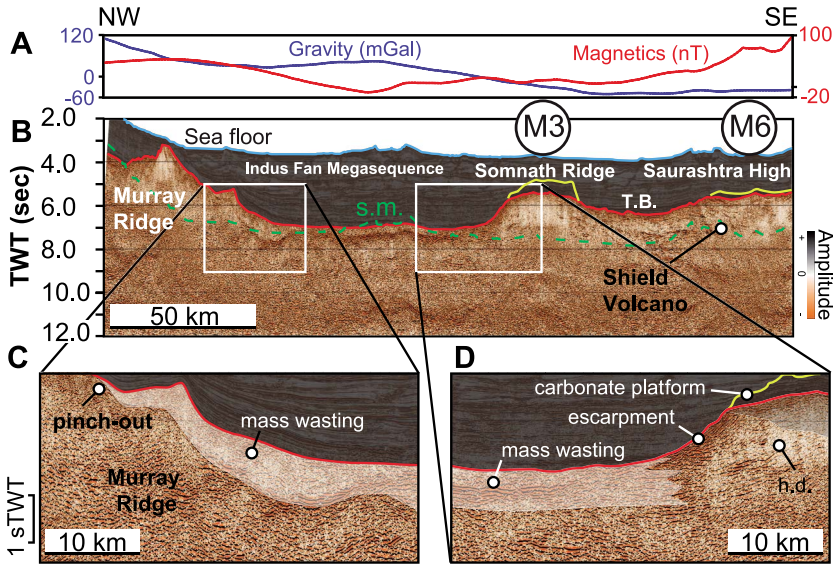

Figure 12. Seismic reflection line (orientation NW–SE). (a) Potential field data, (b) seismic image interpretation of Murray Ridge, Somnath Ridge, and Saurashtra High (green curve is the seabed multiple), (c) volcaniclastic mass-wasting pinch-out on the Murray Ridge, and (d) Somnath Ridge NW escarpment to mass-wasting transition. Note the pinch-out toward the NW of the mass-wasting seismic facies on the proto-Murray Ridge, which was previously described to have been uplifted at 20 Ma [*Mountain and Prell*, 1990]. The seismic facies transition from hyaloclastic delta fringe (h.d.) to mass-wasting deposits is highlighted in Figure 12d. Line location is shown in Figure 6.

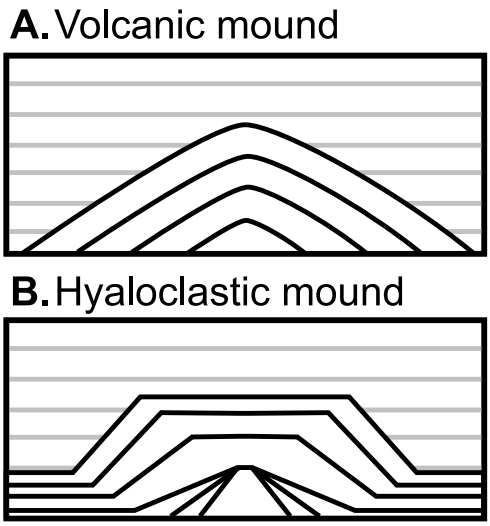

Figure 13. (a) Schematic volcanic mound as defined by *Vail et al.* [1977] and (b) hyaloclastic mound from this study. This scheme can now be used to reevaluate other volcanic provinces and help recognize the characteristic features associated with this type of edifice: the topset geometry and aggradational to progradational pattern of the escarpments.

in the study area (Figure 16b). The bulk of the Somnath Ridge is composed of hyaloclastic mounds and is associated with an elongated gravity low trending NE–SW, whereas the Saurashtra High and shield volcanoes are expressed by rounded gravity highs (Figure 16).

5. Discussion

5.1. Location of the Somnath Ridge in a Plate Model

[41] In the study area, the Somnath Ridge and Saurashtra High occur along a 305 km long zone trending NE–SW and 155 km wide (with an additional 290 km extending into the Indian offshore domain) (Figure 3d). The first question raised by the presence of this isolated volcanic platform located along strike from the main rifting direction of this margin is: why has it developed at this location? The emplacement of this volcanic ridge was interpreted to be related to strike-slip strain accommodation along the continental margin during the separation of the Laxmi Ridge and the Seychelles from India together with the associated volcanism [*Corfield et al.*, 2008].

[42] Here we present a series of regional reconstructions using a global reference frame [*Torsvik et al.*, 2008] corrected for true polar wander [*Steinberger and Torsvik*, 2008]

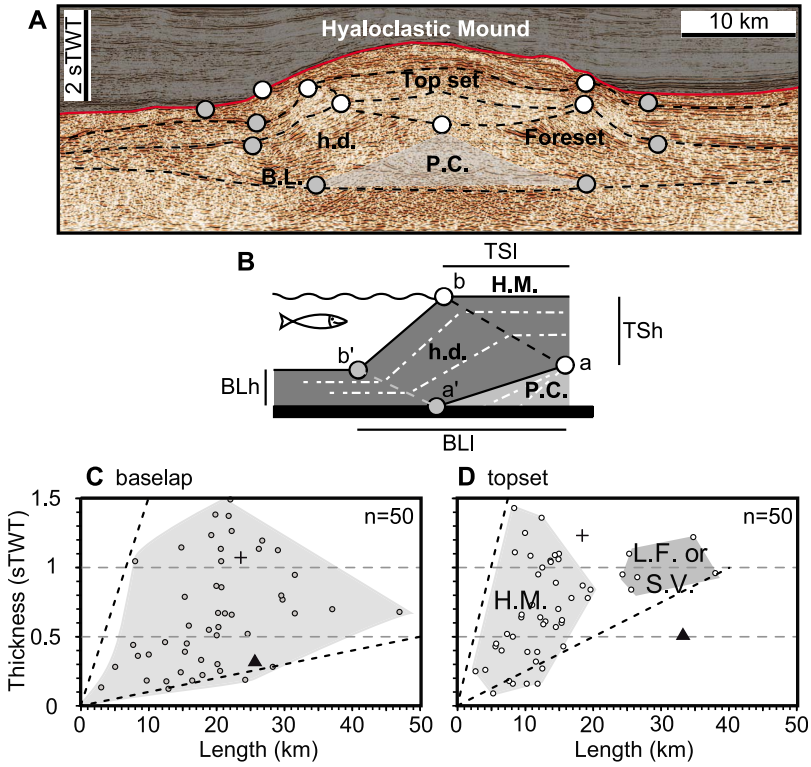

Figure 14. Hyaloclastite delta quantification diagram (see text for details). (a) Descriptive interpreted seismic line of measured elements, (b) schematic diagram of measured elements of volcanic structures, base lap height (BLh) and length (BLl), and top set height (TSh) and length (TSl), (c) length (BLl, km) versus thickness (BLh, sTWT) plot of hyaloclastite delta base lap, and (d) length (TSl, km) versus thickness (TSh, sTWT) plot of hyaloclastite delta topset. Two comparison data points are inserted in Figures 14c and 14d from the Møre Margin (black cross) and the Jan Mayen Fracture Zone (black triangle) (measurements are from *Planke et al.* [2000, Figure 7]). PC, pioneering cone; BL, base lap; hd, hyaloclastite delta; HM, hyaloclastic mound; LF, landward flow; SV, shield volcano.

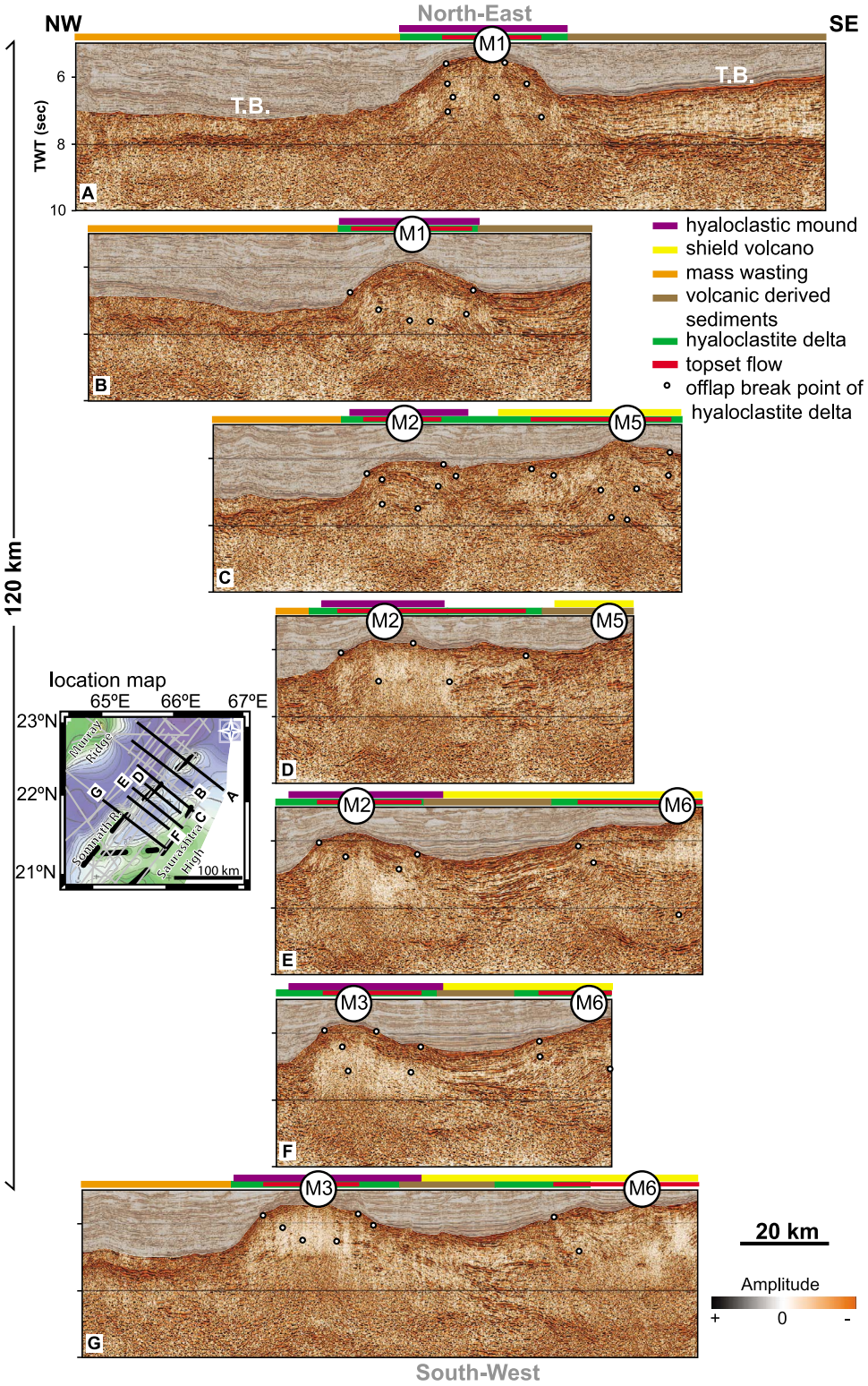

Figure 15. (a–g) NW–SE multiple parallel seismic images along a NE–SW region of 120 km to illustrate the volcanic platform and seismic facies variations within the study area.

where the main tectonic features involved in the mid-Cretaceous to early Cenozoic breakup and early seafloor spreading west of the Indian subcontinent are restored to their paleopositions according to published models and our own interpretation (Figure 17). The Indian Plate is kept in its present day position and all other tectonic elements are shown relative to India. Note that this reconstruction is based on a "moving hotspot" model and results in different

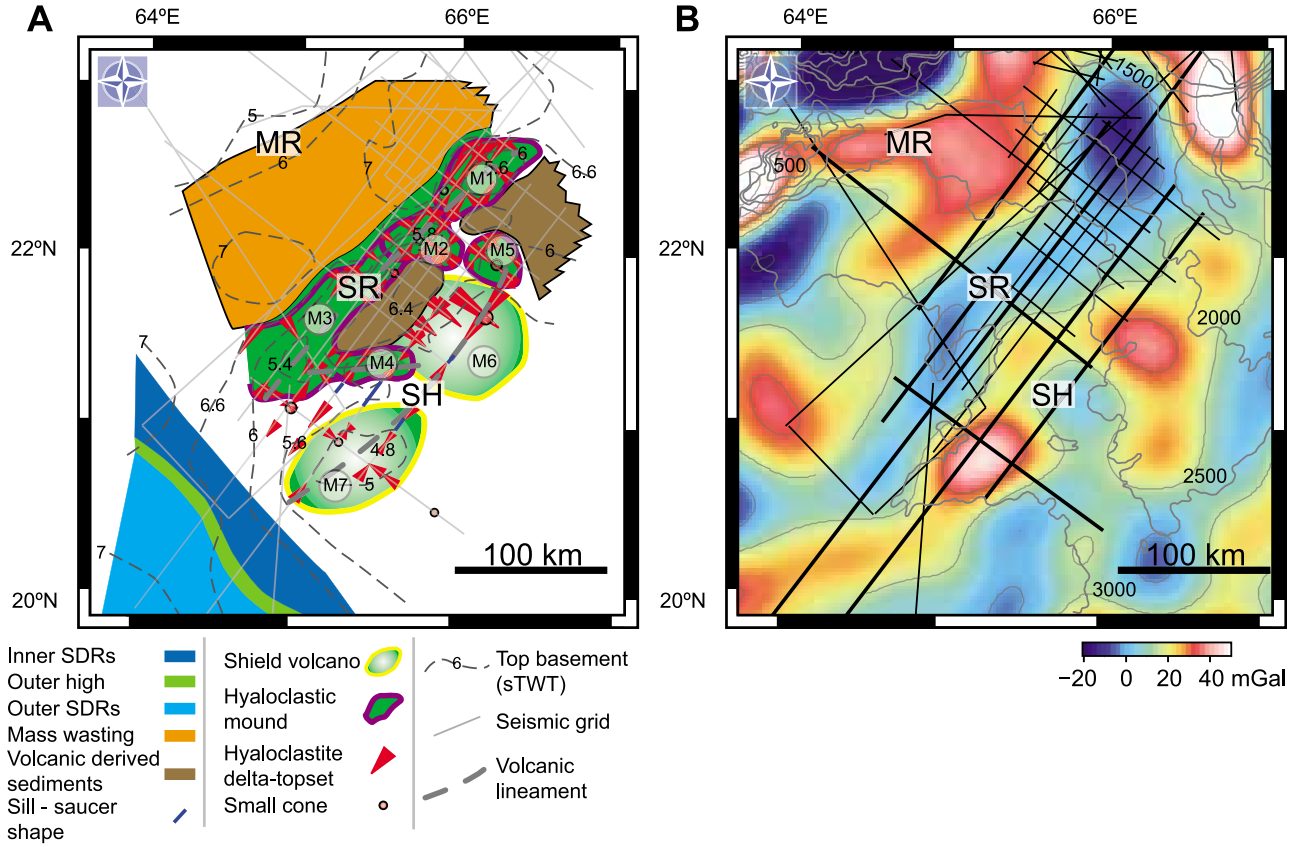

Figure 16. (a) Seismic facies and volcaniclastic features map along the volcanic platform and surrounding areas covered by seismic and (b) Bouguer gravity anomaly filtered 200 km high pass and bathymetric contours. Note the negative gravity signature below the Somnath Ridge and the positive signature below the Saurashtra High and Murray Ridge.

positions of the hotspots relative to the tectonic plates, while other published reconstructions are based on a "fixed hotspot" model.

[43] In our reconstructions we focus on major tectonic events (including breakup, and/or compressional events and proximity to inferred hotspot positions), highlighting the location of the ridges (Figure 17) and magmatism through the period 120–63 Ma (Figure 18). It has been recognized that magmatism associated to Gondwana breakup was taking place in limited, discrete provinces where conditions allowed melt generation [*Norton and Sclater*, 1979; *Mahoney et al.*, 1991; *Storey et al.*, 1995; *Hawkesworth et al.*, 1999; *Courtillot et al.*, 1999].

[44] During Aptian time (~120 Ma, approximately chron M0) the opening of the oceanic Somali Basin ceased, thus marking the end of a rifting event that had initiated in the Jurassic (~153 Ma) between Africa and the Madagascar block [*Rabinowitz et al.*, 1983] (Figure 17a). The Amirante Ridge, Seychelles, Laxmi Ridge, Somnath Ridge, and Murray Ridge are located between the Indian Plate and the oceanic Somali Basin. The southern part of the Indian Plate is located above the Crozet and Marion hotspots (Figure 17a). Magmatism is known to occur later in the eastern part of the Indian Plate at 115 ± 1 Ma, the Rajmahal Traps (Figure 18) [*Kent et al.*, 1997].

[45] At the Albian-Cenomanian transition, ~99 Ma, the Indian-Seychelles block and the Madagascar eastern margin experienced strike-slip motion and a compressional event might have occurred between the northwestern part of the Indian margin and the Madagascar/Somali Basin (Figure 17b). We show the position of the Somnath Ridge just outside the Somali Basin, recognizing its proximity to the inferred region of compression between the African (Nubian)–Madagascar plate and the Western Indian Margin, which is a dextral transform zone from 95–84 Ma along the eastern margin of Madagascar [*Plummer and Belle*, 1995]. At this stage the Somnath Ridge would have overlain an extinct spreading axis within the Somali Basin (SR in Figure 17b).

[46] The mid-Late Cretaceous time recorded in the northwestern Indian Ocean is characterized by a series of events that appear to be related to episode(s) of compression and volcanism. Volcanic activity in the west Indian Ocean during the Turonian-Campanian was proposed based on volcanism in Madagascar described by *Besairie* [1972], and sediments of volcanic origin drilled at the DSDP site 241. Recent studies focused on the northern part of Madagascar show that basaltic magmatism north of Madagascar seems to have had two different origins: in the northwest of the island a N-MORB-like composition indicates shallower sources

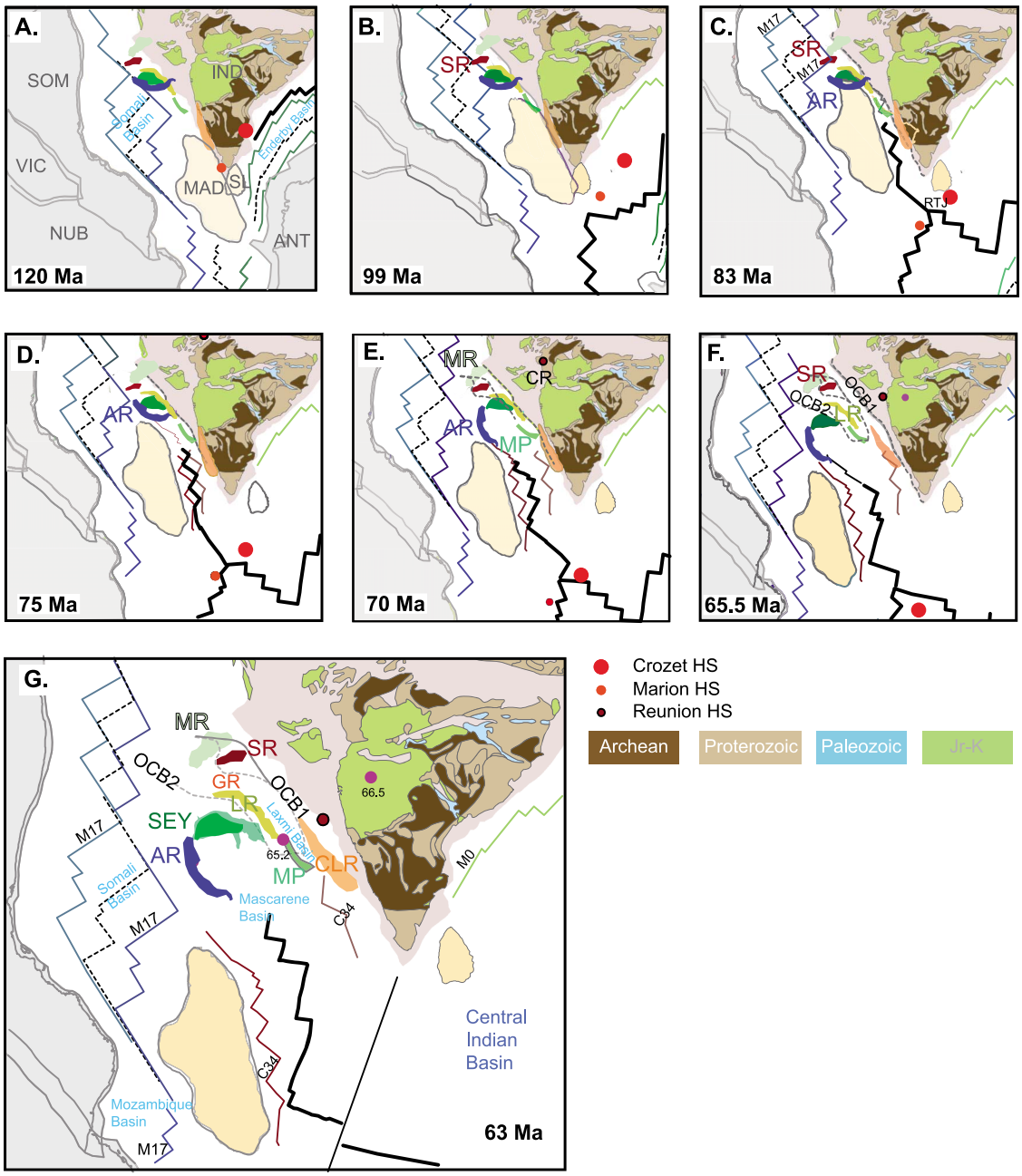

Figure 17. (a–g) Plate organization age model at 120, 99, 83, 75, 70, 65.5, and 63 Ma with Somnath (SR) (brown patches) and Amirante (AR) (blue patches) ridges and hotspot (HS) position (red and purple dots). Note that the colors in Figures 17a–17f correspond to the colors labeled in Figure 17g. Note that the space required to fit AR, SR, MR, SEY, and LR between Madagascar and India is optimal at 75 Ma, which is before the initiation of opening at 71 Ma of the Gop Rift. SOM, Somalia; VIC, Victoria; NUB, Nubia; MAD, Madagascar; SL, Sri Lanka; ANT, Antarctica; RTJ, Ridges Triple Junction; MR, Murray Ridge (light green); GR, Gop Rift; LR, Laxmi Ridge (yellow); CR, Cambay Rift; SEY, Seychelles (bright green); CLR, Chagos-Laccadive Ridge (light orange); MP, Mascarene Plateau (green).

for the Late Cretaceous lava flows and dykes, whereas in the northeast more enriched, high Nb-Ti volcanics indicate a deeper origin [*Melluso et al.*, 2003].

[47] Further away from the Madagascar–western coast of India, within the Eastern African margin, unexplained tectonic events also occurred around Late Cretaceous times. Folding of the Mesozoic cover in SW Somalia (including a Late Cretaceous unconformity) was related by *Boccaletti et al.* [1988] to compressional events in the Indian Ocean. Emplacement of ophiolites onto the eastern margin of Arabia and Pakistan was also attributed to relative motion between India and Madagascar [*Gnos et al.*, 1997].

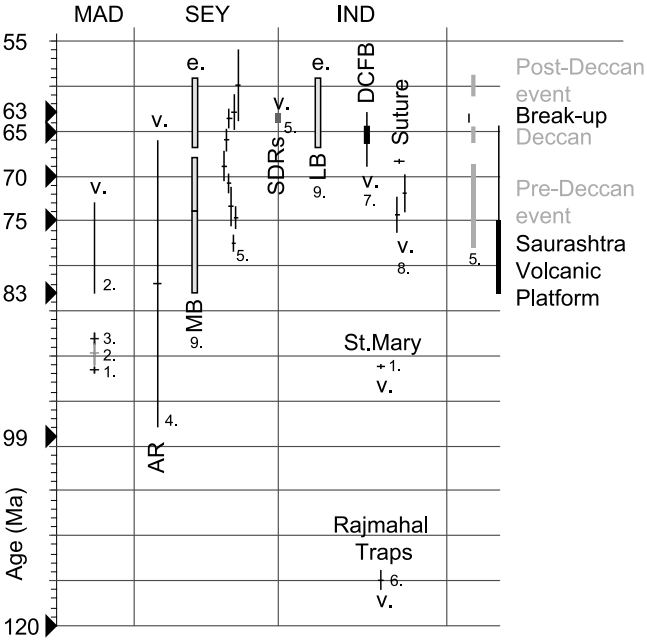

Figure 18. Summary of volcanism (v) in Madagascar (MAD), Seychelles (SEY), India (IND), and their surroundings (vertical bars including age and uncertainties) and extension (e) in Laxmi (LB) and Mascarene Basin (MB) from 120 to 55 Ma. Black arrows correspond to the plate reconstructions that are framed in Figure 17. The proposed time of emplacement of the Saurashtra Volcanic Platform in this study is associated with a potential earlier event predating the Deccan event ~65.5 Ma. References are as follows: 1, *Torsvik et al.* [2000]; 2, *Mahoney et al.* [1991]; 3, *Storey et al.* [1995]; 4, *Fisher et al.* [1968]; 5, *Collier et al.* [2008, and references therein]; 6, *Kent et al.* [1997]; 7, *Courtillot et al.* [1999]; 8, *Robertson and Degnan* [1993] and *Mahoney et al.* [2002]; 9, *Bernard and Munschy* [2000].

Although there are too many uncertainties in the timing and extent of these events, we note that the Late Cretaceous time marked an important turning point in the evolution of western Indian Ocean.

[48] During Turonian time (~88.5–91 Ma in Figure 18 [e.g., *Mahoney et al.*, 1991]), magmatism is recorded in the stratigraphy of the Madagascar sedimentary basins. Equivalent ages of magmatism from Madagascar to SW India (St. Mary, Figure 18) are reported by *Torsvik et al.* [2000], marking the initiation of the breakup between Madagascar and India in that part of the margin.

[49] At the Santonian-Campanian transition (~83 Ma; magnetic anomaly C34) the India-Seychelles block separated from Madagascar with initiation of spreading in the Mascarene Basin (Figure 17c) [*Bernard and Munschy*, 2000]. Although the age of the Amirante Ridge (AR, blue in Figure 17c) formation is not known, we show this feature as part of the Seychelles complex that was part of the Western Indian Margin before rifting between Madagascar and India occurred. In this scenario, the Amirante Ridge would have been located very close to the northern tip of Madagascar, which is problematic. From dredged sediment samples on the edges of the Amirante Ridge (SW of Seychelles block), *Fisher et al.* [1968] dated basalts at 82 ± 16 Ma using K-Ar methods (Figure 18). Volcanism is also recorded SW of Madagascar at ~73–83 Ma (Figure 18) [*Mahoney et al.*, 1991]. We suggest that transpression between the Madagascar-Africa Plate and the Indian Plate between 99 and 83 Ma might have facilitated the creation of both the Amirante Ridge and possibly the Somnath Ridge (SR, brown in Figure 17c). During the opening of the Mascarene Basin (~83 Ma) the Amirante Ridge might have been rotated clockwise and separated from the Seychelles by propagating seafloor spreading (Figures 17c and 17d).

[50] The area of interest covered in this study is the Campanian-Maastrichtian time (~70 Ma; magnetic anomalies C31/C32) characterized by the movement of the Murray Ridge away from the Indian shield (phase of extension?) (MR in light green, Figure 17e). The Amirante Ridge follows the movement of extension of India away from Madagascar. The Mascarene Plateau is offset from the southern part of the Laxmi Ridge. The Laxmi Ridge and Seychelles block are still attached in this reconstitution, which differs from the model suggesting extension between the Seychelles, Laxmi Ridge and India that could have led to the opening of the Laxmi Basin and Gop Rift [*Bhattacharya et al.*, 1994; *Collier et al.*, 2008]. The Cambay Rift (CR in Figure 17e) was located south of the "Réunion" hotspot. Evidence of volcanism at ~71 Ma near offshore Seychelles (including on the West Seychelles Plateau) has been provided by *Plummer and Belle* [1995] (Figure 18). *Collier et al.* [2008] has identified this as the time of the opening of the Gop Rift. However, according to our reconstructions this opening might have occurred slightly after 70 Ma because the position and extent of the Madagascar/Mascarene Basin would have precluded further extension between the Seychelles and the Western Indian Margin at that time. On the northern edge of the Indian Plate (Tethyan Himalaya–Suture in Figure 18), volcanism is also reported at ~68.5 Ma time [*Robertson and Degnan*, 1993; *Mahoney et al.*, 2002], as well as in the Goru Formation (Upper Maastrichtian, minimum age ~70,6 Ma) in the Pab Range SW Pakistan [*Eschard et al.*, 2004]. This occurrence of volcanism north of the study area is consistent with magmatism active around 70.6–65.5 Ma in the study area.

[51] At the time at which the Deccan Traps were being emplaced (~65.5 Ma Maastrichtian-Danian) (Figure 17f), the Somnath Ridge represented the northern boundary of the Greater Deccan Province [*Todal and Edholm*, 1998]. The previously described framework and ocean-continent boundaries defined in this study (OCB 1 and 2, Figures 2 and 16f) are spatially organized at ~65.5 Ma with the identified OCBs at the east and west of the Laxmi Ridge, respectively. The tectonic scheme for the spreading of the Carlsberg Ridge was in place by 63 Ma (Figure 17g) from the ridge jump from the Laxmi Basin and Gop Rift to the zone dividing the Laxmi Ridge and the Seychelles microcontinent thus allowing accretion of oceanic crust [e.g., *Royer et al.*, 2002; *Collier et al.*, 2008; *Minshull et al.*, 2008].

[52] On the basis of the regional plate movements and ages of volcanism, we conclude that the most likely window for development of the Somnath Ridge and the Saurashtra High was between 83 and 75 Ma (Figure 18), which predates the proposed age of pre-Deccan activity between 78 and 71 Ma by *Collier et al.* [2008]. This may have been

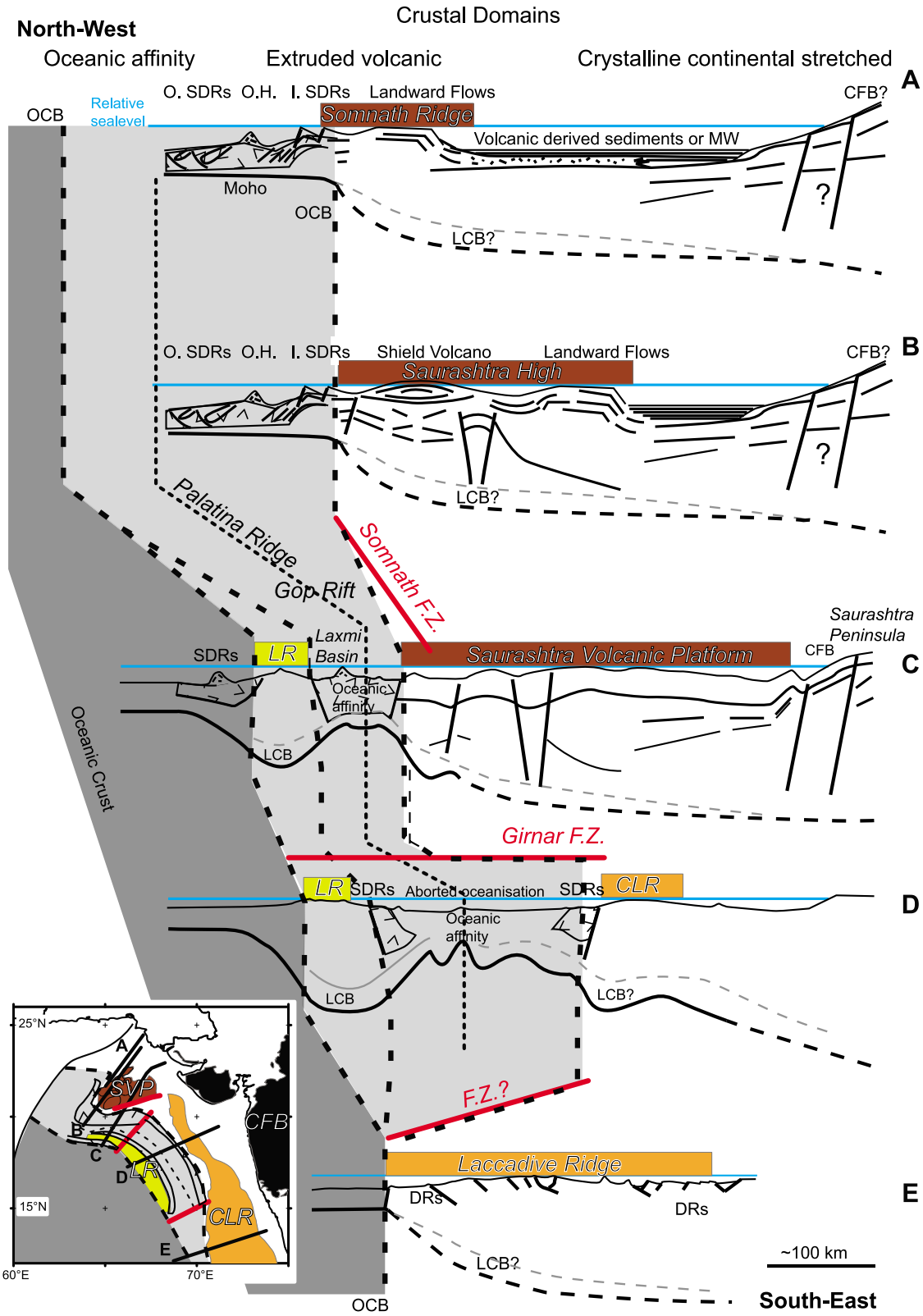
Crustal Domains
North-West
Oceanic affinity
Extruded volcanic
Crystalline continental stretched
A
O. SDRs O.H. I. SDRs Landward Flows
CFB?
OCB
Relative sealevel
Somnath Ridge
Volcanic derived sediments or MW
Moho
OCB
LCB?
B
O. SDRs O.H. I. SDRs Shield Volcano Landward Flows
CFB?
Saurashtra High
LCB?
Palatina Ridge
Somnath F.Z.
Gop Rift
Saurashtra Peninsula
SDRs
LR
Laxmi Basin
Saurashtra Volcanic Platform
CFB
C
Oceanic affinity
LCB
Oceanic Crust
Girnar F.Z.
LR
SDRs
Aborted oceanisation
SDRs
CLR
D
Oceanic affinity
LCB
LCB?
F.Z.?
Laccadive Ridge
DRs
DRs
E
LCB?
~100 km
OCB
South-East
25°N
15°N
60°E
70°E
A
B
C
D
E
SVP
LR
CLR
CFB

Figure 19

caused by a combination of compression features that were later reactivated during the breakup of the Western Indian Margin, synchronous with development of extensive SDRs. Other factors such as extension or a mantle plume [*White*, 1992] can represent potential contributors associated to this major volcanic event. Volcanism could have started at this time and continued after 83 Ma, right up to the emplacement of Deccan volcanism onshore at ~65 Ma [e.g., *Mahoney*, 1988]. This in turn predates the breakup between the Seychelles and India at ~63 Ma (Figure 17g).

5.2. Margin Segmentation and the Location of Volcanism

[53] Segmentation of margins has been documented since the early 1980s [e.g., *Keen and Beaumont*, 1990]. The role that transform faults may play in breakup style has recently been linked to the location of volcanic events within the breakup process (e.g., SDRs, volcanic ridges). Along the Atlantic margins, different authors show that margin segmentation is important along strike in controlling the type of volcanic processes and the organization of deposits [e.g., *Franke et al.*, 2007; *Elliott and Parson*, 2008; *Hirsch et al.*, 2008].

[54] The western Indian rifted margin is classified as a type of transform volcanic margins. *Malod et al.* [1997] recognized three main transform faults: (1) Somnath Fault Zone south of the Saurashtra volcanic platform, (2) Girnar Fracture Zone running from north of the Laxmi Basin to the west of the Laxmi Ridge, and (3) an unnamed fracture zone south of the Laxmi Basin (red lines in Figure 19). To illustrate the segmented margin organization we have plotted a series of across-margin profiles (Figure 19), starting in the northwest with the Somnath Ridge and extending to the southeast as far as the volcanic Laccadive Ridge. These profiles illustrate how these three main tectonic lineations (fault zones) bound the geometry of the rifted margin. To the North of the Somnath Fault Zone, the Saurashtra volcanic platform (brown bar in Figures 18a–18c) developed extensive volcanic edifices with volcanic sediments or mass-wasting deposits onlapping landward toward the rifted margin. To the south of Somnath Fault Zone the Gop Rift is bounded by the Girnar Fault Zone (Figure 19c). The volcanism expressed there is mostly in the form of extensive SDRs, continuous with those observed southwest of the Somnath Ridge (Figures 19a and 19b). South of the Gop Rift the Laxmi Basin (aborted oceanic rift) shows SDRs on both sides (Figure 19d). The margin's final segment occurs south of the unnamed Fracture Zone and corresponds to the Laccadive Ridge, which developed along the track of the Réunion hotspot after the main onshore Deccan emplacement event (Figure 19e).

[55] The location of the Saurashtra Volcanic Platform could be related to a structural lineation following previous structures inherited from the separation of Madagascar and India. The NE–SW present-day orientation of the Somnath Ridge could indicate a lineation parallel to other observed fault zones further south along the West Indian Margin.

[56] The transform/strike slip component of these lineations will require analysis of more data from a deep-focused seismic survey or a regional stress analysis on outcropping pre-Deccan event geological structures.

5.3. Stages of Edifice Evolution

[57] From our mapping of the Somnath Ridge and Saurashtra High volcanic buildups we can spatially and vertically analyze the organization of the different facies and edifices in order to outline the main evolutionary stages. As shown in Figures 13–15 the bases of the hyaloclastic mounds in the Somnath Ridge are composed of "basal" cones that we can consider as "pioneering cones" and the first extrusive volcanism in the study area. Over this more effusive material, bigger hyaloclastic mounds were constructed with topsets and delta foresets largely composed of lava basalts and brecciated volcanic rocks. The area northeast the Somnath Ridge and Saurashtra High are composed of massive landward flows (mostly hyaloclastic mounds) which in the model of *Planke et al.* [2000] are related to the infill of a broad basin (Figures 7 and 8a). Compared to other subsurface examples in the NE Atlantic (20 km long maximum and ~3 km thick), the thickness here ranges from 2.4 to 9.6 km and the areal extent is >30 km. The southwest portion of the volcanic platform shows the development of isolated (M7) or composite (M6) shield volcanoes (Figures 10 and 15g). The position of the most seaward shield volcano (M7) may be related to one of the last stages of volcanism, paralleling the development of the inner SDRs (Figures 9b and 15g). From this we can outline four development stages: (1) initiation of volcanism by pioneering cones (subaerial to subaqueous), (2) extrusion of massive volumes of lavas (subaerial) and hyaloclastites infilling basins (subaerial to subaqueous) and building the mounds and ridges, (3) seaward development of shield volcanoes (subaerial to subaqueous), and (4) development of SRDs (marine) that are potentially related to the beginning of seafloor spreading. The exclusive presence of saucer-shaped sills within the volcaniclastic sediments and hyaloclastic mounds or shield volcanoes and absence of intrusions in the overlying Indus Fan Megasequence differs from other well-known volcanic margins (e.g., NE Atlantic, Australia NW Shelf) where extensive magmatic intrusive complexes are observed in the overlying sedimentary succession. This is consistent with the fact that no phase of

Figure 19. (a–e) Crustal-scale sketches along the west Indian rifted margin with potential location of volcanic edifices, types, and major tectonic domains. The three main transform faults/fault zones (FZ) are labeled in red in the crustal sketches and on the map. Oceanic crustal domains and areas of oceanic affinity are shaded in dark grey and light grey, respectively, locally bounded by SDRs that mark the ocean-continent boundaries. Location map: CFB, continental flood basalt (black); SVP, Saurashtra volcanic platform (brown) made of Somnath Ridge (SR) and Saurashtra High (SH); LR, Laxmi Ridge (yellow); CLR, Chagos-Laccadive Ridge (light orange); LCB, lower crustal body; DR, dipping reflectors; I. SDRs, Inner SDRs; O.H., Outer High; O. SDRs, Outer SDRs. Figures 19a and 19b are from this study; Figures 19c–19e are from Directorate General of Hydrocarbons–India, E&P report 2006–2007, (available at http://www.dghindia.org/pdf/2006-07.pdf).

Table 3. Geometrical Extraction Along Seismic Profiles and Budget of the Volcaniclastics[a]

Volcanic Edifice	Volume (10^3 km^3)	Volume Uncertainty (%)	Scenario 1 Life Span (Myr)			Scenario 2 Life Span (Myr)			Scenario 3 Life Span (Myr)		
			Volcanoes Oceanic Setting	Deviation Plus	Deviation Minus	Volcanoes Continental Crust	Deviation Plus	Deviation Minus	Flood Basalts	Deviation Plus	Deviation Minus
M1	13.1	7	0.469	0.102	0.071	2.988	0.664	0.460	0.015	0.004	0.105
M2	7.7	>1	0.274	0.059	0.041	1.741	0.387	0.268	0.009	0.002	0.061
M3	39.6	3	1.413	0.307	0.214	8.991	1.998	1.383	0.044	0.013	0.316
M4	4.1	2	0.147	0.032	0.022	0.938	0.208	0.144	0.005	0.001	0.033
M4 u.e.	1.5	2	0.054	0.012	0.008	0.346	0.077	0.053	0.002	0.000	0.012
M5	8.3	2	0.297	0.065	0.045	1.889	0.420	0.291	0.009	0.003	0.066
M5 u.e.	2.7	2	0.095	0.021	0.014	0.605	0.135	0.093	0.003	0.001	0.021
M6	49.3	>1	1.760	0.383	0.267	11.201	2.489	1.723	0.055	0.016	0.393
M6 u.e.	12.9	>1	0.461	0.100	0.070	2.931	0.651	0.451	0.014	0.004	0.103
M7	16.1	14	0.574	0.125	0.087	3.652	0.812	0.562	0.018	0.005	0.128
M7 u.e.	8.7	16	0.310	0.067	0.047	1.971	0.438	0.303	0.010	0.003	0.069

[a]Upper edifice, u.e.

intrusive volcanism has so far been recorded within the Indus Fan Megasequence.

5.4. Estimation of Volcanic Rock Volumes and Extrusion History

[58] In this section we attempt to present volumetric estimates of the observed edifices and volcanic extrusion life span, through comparison with published compilations of volcanic output rates equivalent to the setting of this study. All these results are explained in this section and are summarized in Table 3. It is important to note that we do not take into account volumes intruded into the crust and lower crustal bodies because we are not able to calibrate those with our data.

5.4.1. Volumes of Volcanism

[59] We estimate volumes on the basis of the subsurface extent of the different volcanic domains with assessment of the uncertainties related to the seismic interpretation and depth conversion of the base of each edifice by isopach computation. The time-depth conversion in this type of volcanic extruded material is acknowledged to be highly anisotropic and thus prone to uncertainties [*Planke and Eldholm*, 1994]. Interval velocities are estimated at each location using the known stratigraphic organization and show values ranging from ~4 km/s to >6 km/s below the top basement reflection (Figure 4c and 8). For example, variation of 0.5 km/s in the interval velocity of hyaloclastic mound M4 causes a variation of 5–10% in the resulting volume.

[60] We obtain volumes for the extruded volcanic material ranging from $1.5 \pm 0.03 \times 10^3$ km^3 (M4 upper edifice) to $49.3 \pm 0.37 \times 10^3$ km^3 (M6) (Figure 20a). In comparison with published volumes from volcanic margins or oceanic volcanic provinces (e.g., Faroe Islands, Réunion, Hawaii), we can suggest volumetric parallels between the edifices observed in the present study and these other volcanic provinces. Mound 4 is volumetrically equivalent to Réunion or the Faroe Islands volcanoes, whereas Mound 7 is equivalent to Kilauea and Mound 6 to Mauna Loa in volume (Figure 20a). Compared to the volumetric estimation of the Great Deccan Province ~1.8×10^6 km^3 (surface ~1.8×10^6 km^2) [*Todal and Edholm*, 1998] or the Deccan Traps 1.3×10^6 km^3 [e.g., *Jay and Widdowson*, 2008] (Figure 20b, surface ~5×10^5 km^2 [e.g., *Mahoney*, 1988]), assuming preserved (i.e., noneroded as present day) volumes, the total volume represented by the study area edifices can be estimated to range from 1.38×10^5 km^3 to 1.79×10^5 km^3. If we project these estimations to the entire Saurashtra volcanic platform (Pakistan and Indian offshore area), it could represent a volume up to 3.45×10^5 km^3 (Figure 20b, surface ~4.4×10^4 km^2). This volume is a minimum estimate of the total amount of volcaniclastic rock present on the margin because we are not including the SDRs or the subaerial SDRs extruded in the Gop Rift and Laxmi Basin. We therefore calculate that the offshore volcanic rocks described here are equivalent to ~19 or 26.5% of the volume of the Great Deccan Province (1.8×10^6 km^3 [*Todal and Edholm*, 1998]) or the Deccan Flood Basalts (1.5×10^6 km^3 [*Eldholm and Coffin*, 2000]), respectively (Figure 20b).

[61] When compared to a compilation of surface-volume data for world LIPs from the Pacific Ocean, Indian Ocean, North and South Atlantic with their Continental Flood Basalts (Figure 20b), it is evident that the Saurashtra Volcanic Platform represents a significant volume of magma extruded to the Earth surface that can now be added to the budget of the Great Deccan Large Igneous Province.

5.4.2. Life Span Estimate of Volcanic Activity

[62] To estimate the volcanic extrusion life span of the study area we use values of volumetric, time averaged volcanic output rates (Qe) from *Crisp* [1984] updated by *White et al.* [2006] because we are dealing with volcanic edifices (seismic scale) rather than identified individuals lava flows (outcrop scale). We do not use the values obtained from onshore Deccan studies [e.g., *Chenet et al.*, 2008] of 30–200 km^3/yr because we do not have the same detailed time and/or geometrical constrains that their studies have for single lava flows/events. We use time-averaged Qe from three different geological settings [*White et al.*, 2006]: (1) for volcanoes in oceanic settings $2.8 \pm 0.5 \times 10^{-2}$ km^3/a, (2) for volcanoes on continental crust $4.4 \pm 0.8 \times 10^{-3}$ km^3/a, and (3) for flood basalts of $9 \pm 2 \times 10^{-1}$ km^3/a. If we use the two first output rates (volcanoes on oceanic or continental crust), the life span of the individual volcanic buildups along the west Indian rifted margin range from 0.1 to 1.8 Myr and 0.3 to 11.2 Myr, respectively. For the continental flood basalt scenario, the life span drops significantly to very short periods of 0.003–

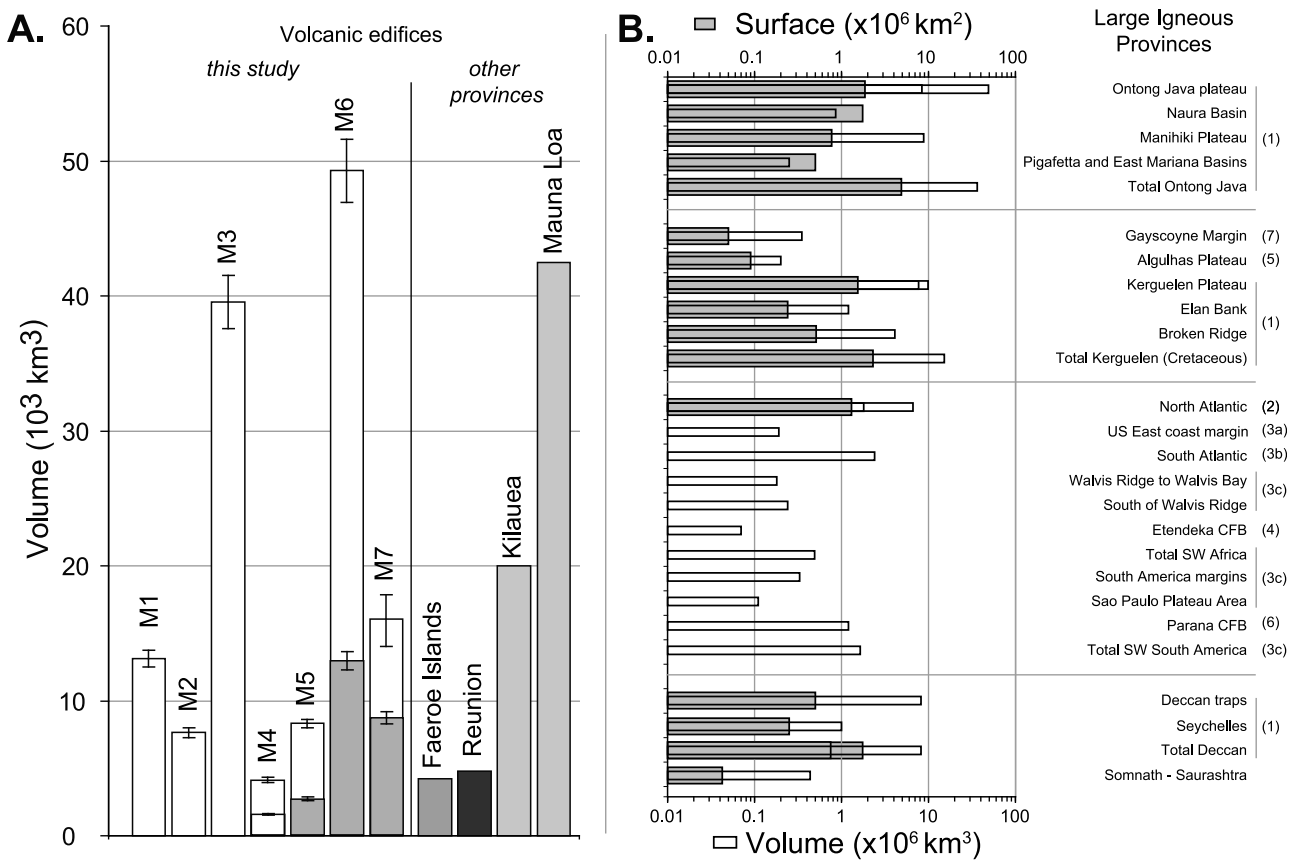

Figure 20. (a) Volume estimation of edifices along the Somnath Ridge and the Saurashtra High compared to the Faroe Islands, Réunion, and Hawaiian volcanoes (values of *White et al.* [2006]). Calculation of volumes is explained in the text. (b) Surface area and volume of other large igneous provinces (oceanic and continental flood basalt) from various sources for comparison with this present study. Sources are listed as follows: 1, *Coffin and Eldholm* [1994]; 2, *Eldholm and Grue* [1994]; 3a, *Gladczenko* [1994]; 3b, *Gladczenko et al.* [1997]; 3c, *Gladczenko et al.* [1998]; 4, *Milner et al.* [1992]; 5, *Parsiegla et al.* [2008]; 6, *Peate et al.* [1990]; 7, *Rey et al.* [2008]).

0.05 Myr (Table 3). On the basis of the three different Qe values, the Somnath Ridge alone (M1-4) would have needed 3.36 ± 0.7, 21 ± 4.7, and 0.1–0.85 Myr to be formed. The entire Saurashtra volcanic platform would have needed between 12.3 ± 2.7, 78 ± 17.4 to 0.38–3.13 Myr to be emplaced.

[63] Combining the volcanic life span estimates with the plate reconstitution (Figure 17) development of the volcanic platform (Somnath Ridge and Saurashtra High) could have occurred in a broad 75–65.5 Ma window (Scenario 1: volcanism in an oceanic setting). Alternatively, if the bulk of the volcanism was related only to an early and short development phase, it could have occurred between 75 to 71 Ma (Scenario 3: flood basalts). Therefore the volcanism offshore in the study area could be associated with either Qe characteristics of volcanism in an oceanic setting (Scenario 1) or flood basalts (Scenario 3). We conventionally assume the top basement reflection to be regionally associated to the last rifting event, the Deccan event, so we favor Scenario 1 (75–65.5 Ma). The only potential way of testing this hypothesis will be to date drilled samples of the basalts below the top basement in the area. Nevertheless, in the North Atlantic volcanic province, episodic volcanism leading to seamounts in the Rockall Trough is recognized to occur in multiple pulses of activity ~1 to 2 Myr long over a period of time between 5 to 10 Myr prior to breakup [*O'Connor et al.*, 2000]. This is equivalent timing to the proposed Scenario 1 in the study area.

6. Conclusions

[64] The following conclusions can be made from this study.

[65] 1. The present study of the western Indian rifted margin is consistent with recent work on other volcanic rifted margins, and illustrates the lateral variability of the volcanostratigraphic framework and the high diversity of geometries seen in the volcanic basement caused by the development of rifted margins during the onset of oceanic spreading.

[66] 2. We present a complete analysis of the different crustal domains of the NW Indian Ocean and have found areas ranging from the Indo-Pakistani continental stretched crust, through the transitional crust with extruded volcanics,

to the oceanic crust. The potential heritage of multiple rifting events before the spreading and accretion of ocean crust at 63 Ma could date back as far as the opening of the Somali Basin off the East coast of Africa during the Jurassic at ~153 Ma. The multiple rifting might have started before the Mascareine Basin opening (pre–83 Ma).

[67] 3. The Somnath Ridge and Saurashtra High are buried below sediments of the Indus Fan and are composed of different volcanostratigraphic edifices recognized on seismic reflection data and potential field data. The main volcanic sequence and architecture constitutes a style similar to the volcanic margins of the Northeast Atlantic.

[68] 4. A number of seismic volcanostratigraphic facies and geometric architectural styles have been identified and illustrated in the study area. The edifices are clearly identified, and comprise hyaloclastic mounds and shield volcanoes of various sizes. A significant lateral deposition of volcanic sediments or mass wasted sediments surround the different edifices. The size and volume of these volcanic constructions are comparable to volcanic edifices at the surface such as the Faroe Islands, La Réunion, and Hawaiian volcanoes as Kilauea and Mauna Loa. The recognition of individual volcanic edifices on other volcanic margins should be reevaluated in the light of the present study.

[69] 5. The emplacement of the volcanic platform on the NW part of the Indo-Pakistani Margin seems to be controlled by structures inherited from older known rifting events during the opening of the Indian Ocean. A series of lineations (fault zones) oriented perpendicular to the margin has allowed the focus of melt to be localized in the study area.

[70] 6. The total volume of the Saurashtra volcanic platform (3.45×10^5 km^3 over a surface area of ~4.4×10^4 km^2) represents 19.0–26.5% of the West Indian Volcanic Province (Deccan Traps before erosion). Thus making the West Indian Volcanic Province a significantly bigger LIP than previously known.

[71] 7. Using the volumes of the edifices and the bulk volcanic platform with different volcanic production rates, we have estimated the potential life span of the volcanic activity in the study area. We found that it could have ranged from <1 Myr if the effusive rate from other flood basalts provinces is applicable to <15 Myr based on volcanoes in an oceanic settings.

[72] 8. Using plate reconstructions of the evolution of the West Indian Margin and estimates of the life span of volcanism, from volume production rates of equivalent eruptive systems, we propose two possible scenarios for volcanic emplacement. We favor a scenario of development of the volcanism during the Campanian to Maastrichtian-Danian times (~75 to 65.5 Ma) in an oceanic setting. Likewise, the initiation of volcanism can be potentially related to the opening of the northern part of the west Indian rifted margin along transform faults starting at ~75 Ma, and prolonged in the south to ~71 Ma by the opening of the Gop Rift and the Laxmi Basin with associated volcanism. This makes the window of volcanism longer than previously known in this area, extending from 75 to 63 Ma.

[73] Further calibration of this subsurface volcanic province will be required to confirm some of the outcomes of this study and will necessitate scientific drilling operations or access to industrial exploration samples.

[74] **Acknowledgments.** The College of Physical Sciences and University of Aberdeen are thanked for funding G.C.'s Ph.D. research. We also thank Shell and the NIO-Pakistan for the main seismic reflection data set, C. Gaedicke for the Sonne122 2-D seismic reflection survey (BGR), and R. Edwards and T. Minshull from NOC-Southampton for the 2-D survey CD144 between Saurashtra High and south of Laxmi Ridge. Landmark and SMT Kingdom are thanked for their Software University Grants, which have allowed this work to take place. Figures and filtering operation would not have been possible without the Generic Mapping Tools [*Wessel and Smith*, 1995]. Thanks to Malcolm J. Hole for his time shared on descriptive magmatism and hyaloclastic systems. We are grateful for reviews from Cathy Busby, the anonymous Associate Editor, and the Editor André Revil, which helped to improve the paper.

References

Antobreh, A. A., J. I. Faleide, F. Tsikalas, and S. Planke (2009), Rift-shear architecture and tectonic development of the Ghana margin deduced from multichannel seismic reflection and potential field data, *Mar. Pet. Geol.*, *26*(3), 345–368, doi:10.1016/j.marpetgeo.2008.04.005.

Archer, S. G., S. C. Bergman, J. Iliffe, C. M. Murphy, and M. Thornton (2005), Palaeogene igneous rocks reveal new insight into the geodynamic evolution and petroleum potential of the Rockall Trough, NE Atlantic Margin, *Basin Res.*, *17*(1), 171–201, doi:10.1111/j.1365-2117.2005.00260.x.

Barrère, C., J. Ebbing, and L. Gernigon (2009), Offshore prolongation of Caledonian structures and basement characterisation in the western Barents Sea from geophysical modeling, *Tectonophysics*, *470*(1–2), 71–88, doi:10.1016/j.tecto.2008.07.012.

Bernard, A., and M. Munschy (2000), Le bassin des Mascareignes et le bassin de Laxmi (ocean Indien occidental) se sont-ils formes a l'axe d'un meme centre d'expansion?: Were the Mascarene and Laxmi Basins (western Indian Ocean) formed at the same spreading centre?, *C. R. Acad. Sci., Ser. IIa*, *330*(11), 777–783, doi:10.1016/S1251-8050(00)00221-4.

Berndt, C., S. Planke, E. Alvestad, F. Tsikalas, and T. Rasmussen (2001), Seismic volcanostratigraphy of the Norwegian Margin: Constraints on tectonomagmatic break-up processes, *J. Geol. Soc.*, *158*(3), 413–426, doi:10.1144/jgs.158.3.413.

Besairie, H. (1972), Géologie de Madagascar, 1. Les terrains sédimentaires, *Ann. Geol. Madagascar*, *35*, 1–463.

Bhattacharya, G. C., A. K. Chaubey, G. P. S. Murty, K. Srinivas, K. V. L. N. S. Sarma, V. Subrahmanyam, and K. S. Krishna (1994), Evidence for seafloor spreading in the Laxmi Basin, northeastern Arabian Sea, *Earth Planet. Sci. Lett.*, *125*(1–4), 211–220, doi:10.1016/0012-821X(94)90216-X.

Blakely, R. J. (1995), *Potential Theory in Gravity and Magnetic Applications*, 464 pp., Cambridge Univ. Press, New York, doi:10.1017/CBO9780511549816.

Boccaletti, M., P. Dainelli, A. Angelucci, M. A. Arush, M. M. Cabdulqaadifl, P. Nafissi, G. Picco, and W. E. Robba (1988), Folding of the Mesozoic cover in SW Somalia: A compressional episode related to the early stages of Indian Ocean evolution, *J. Pet. Geol.*, *11*, 157–168, doi:10.1111/j.1747-5457.1988.tb00810.x.

Boldreel, L. O., and M. S. Andersen (1994), Tertiary development of the Faeroe-Rockall Plateau based on reflection seismic data, *Bull. Geol. Soc. Den.*, *41*, 162–180.

Calvès, G. (2009), Tectono-stratigraphic and climatic record of the Arabian Sea, Ph.D. thesis, 292 pp., Univ. of Aberdeen, Aberdeen, U. K., 19 March.

Calvès, G., P. D. Clift, and A. Inam (2008), Anomalous subsidence on the rifted volcanic margin of Pakistan: No influence from Deccan plume, *Earth Planet. Sci. Lett.*, *272*(1–2), 231–239, doi:10.1016/j.epsl.2008.04.042.

Chaubey, A. K., G. C. Bhattacharya, G. P. S. Murty, K. Srinivas, T. Ramprasad, and D. G. Rao (1998), Early Tertiary seafloor spreading magnetic anomalies and paleo-propagators in the northern Arabian Sea, *Earth Planet. Sci. Lett.*, *154*(1–4), 41–52, doi:10.1016/S0012-821X(97)00178-7.

Chaubey, A. K., D. Gopala Rao, K. Srinivas, T. Ramprasad, M. V. Ramana, and V. Subrahmanyam (2002), Analyses of multichannel seismic reflection, gravity and magnetic data along a regional profile across the central-western continental margin of India, *Mar. Geol.*, *182*(3–4), 303–323, doi:10.1016/S0025-3227(01)00241-9.

Chenet, A.-L., F. Fluteau, V. Courtillot, M. Gérard, and K. V. Subbarao (2008), Determination of rapid Deccan eruptions across the Cretaceous-Tertiary boundary using paleomagnetic secular variation: Results from a 1200-m-thick section in the Mahabaleshwar escarpment, *J. Geophys. Res.*, *113*, B04101, doi:10.1029/2006JB004635.

Clift, P. D., C. Gaedicke, R. Edwards, J. Il Lee, P. Hildebrand, S. Amjad, R. S. White, and H. E. Schlater (2002), The stratigraphic evolution of the

Indus Fan and the history of sedimentation in the Arabian Sea, *Mar. Geophys. Res.*, *23*(3), 223–245, doi:10.1023/A:1023627123093.
Coffin, M. F., and O. Eldholm (1993), Scratching the surface: Estimating dimensions of large igneous provinces, *Geology*, *21*, 515–518, doi:10.1130/0091-7613(1993)021<0515:STSEDO>2.3.CO;2.
Coffin, M. F., and O. Eldholm (1994), Large igneous provinces: Crustal structure, dimensions, and external consequences, *Rev. Geophys.*, *32*(1), 1–36, doi:10.1029/93RG02508.
Collier, J. S., V. Sansom, O. Ishizuka, R. N. Taylor, T. A. Minshull, and R. B. Whitmarsh (2008), Age of Seychelles–India break-up, *Earth Planet. Sci. Lett.*, *272*(1–2), 264–277, doi:10.1016/j.epsl.2008.04.045.
Corfield, R., S. Carmichael, J. Bennett, S. Akhter, and M. Fatimi (2008), Break-up history of a volcanic margin: Western India and Pakistan, paper presented at Rifts Renaissance: Stretching the Crust and Extending Exploration Frontiers, Pet. Group, Soc. for Sediment. Geol., Houston, Tex.
Courtillot, V., C. Jaupart, I. Manighetti, P. Tapponnier, and J. Besse (1999), On causal links between flood basalts and continental breakup, *Earth Planet. Sci. Lett.*, *166*(3–4), 177–195, doi:10.1016/S0012-821X(98)00282-9.
Courtillot, V., Y. Gallet, R. Rocchia, G. Féraud, E. Robin, C. Hofmann, N. Bhandari, and Z. G. Ghevariya (2000), Cosmic markers, 40Ar/39Ar dating and paleomagnetism of the KT sections in the Anjar Area of the Deccan large igneous province, *Earth Planet. Sci. Lett.*, *182*(2), 137–156, doi:10.1016/S0012-821X(00)00238-7.
Crisp, J. A. (1984), Rates of magma emplacement and volcanic output, *J. Volcanol. Geotherm. Res.*, *20*(3–4), 177–211, doi:10.1016/0377-0273(84)90039-8.
Deptuck, M. E., G. S. Steffens, M. Barton, and C. Pirmez (2003), Architecture and evolution of upper fan channel-belts on the Niger Delta slope and in the Arabian Sea, *Mar. Pet. Geol.*, *20*(6–8), 649–676, doi:10.1016/j.marpetgeo.2003.01.004.
de Voogd, B., S. P. Palomé, A. Hirn, P. Charvis, J. Gallart, D. Rousset, J. Dañobeitia, and H. Perroud (1999), Vertical movements and material transport during hotspot activity: Seismic reflection profiling offshore La Réunion, *J. Geophys. Res.*, *104*, 2855–2874, doi:10.1029/98JB02842.
Droz, L., and G. Bellaiche (1991), Seismic facies and geologic evolution of the central portion of the Indus Fan, in *Seismic Facies and Sedimentary Processes of Submarine Fans and Turbidites Systems*, edited by P. Weimer and M. H. Link, pp. 383–401, Springer, New York.
Duncan, R. A. (1990), The volcanic record of the Réunion hotspot, *Proc. Ocean Drill. Program Sci. Results*, *115*, 3–10, doi:10.2973/odp.proc.sr.115.206.1990.
Eagles, G., and M. König (2008), A model of plate kinematics in Gondwana breakup, *Geophys. J. Int.*, *173*(2), 703–717, doi:10.1111/j.1365-246X.2008.03753.x.
Edwards, R. A., T. A. Minshull, and R. S. White (2000), Extension across the Indian-Arabian plate boundary: The Murray Ridge, *Geophys. J. Int.*, *142*(2), 461–477, doi:10.1046/j.1365-246x.2000.00163.x.
Edwards, R. A., T. A. Minshull, E. R. Flueh, and C. Kopp (2008), Dalrymple Trough: An active oblique-slip ocean–continent boundary in the northwest Indian Ocean, *Earth Planet. Sci. Lett.*, *272*(1–2), 437–445, doi:10.1016/j.epsl.2008.05.007.
Eldholm, O., and M. F. Coffin (2000), Large igneous provinces and plate tectonics, in *The History and Dynamics of Global Plate Motions*, *Geophys. Monogr. Ser.*, vol. 121, edited by M. A. Richards, R. G. Gordon, and R. D. van der Hilst, pp. 309–326, AGU, Washington, D.C.
Eldholm, O., and K. Grue (1994), North Atlantic volcanic margins: Dimensions and production rates, *J. Geophys. Res.*, *99*, 2955–2968, doi:10.1029/93JB02879.
Elliott, G. M., and L. M. Parson (2008), Influence of margin segmentation upon the break-up of the Hatton Bank rifted margin, NE Atlantic, *Tectonophysics*, *457*(3–4), 161–176, doi:10.1016/j.tecto.2008.06.008.
Emery, D., and K. J. Myers (1996), *Sequence Stratigraphy*, 297 pp., doi:10.1002/9781444313710, Blackwell Sci., Oxford, U.K.
Eschard, R., E. Albouy, F. Gaumet, and A. Ayub (2004), Comparing the depositional architecture of basin floor fans and slope fans in the Pab Sandstone, Maastrichtian, Pakistan, in *Confined Turbidite Systems*, edited by S. A. Lomas and P. Joseph, *Geol. Soc. Spec. Publ.*, *222*, 159–185.
Fisher, R. L., C. G. Engel, and T. W. C. Hilde (1968), Basalts dredged from the Amirante ridge, western Indian ocean, *Deep Sea Res. Oceanogr. Abstr.*, *15*(5), 521–534, doi:10.1016/0011-7471(68)90061-2.
Franke, D., S. Neben, S. Ladage, B. Schreckenberger, and K. Hinz (2007), Margin segmentation and volcano-tectonic architecture along the volcanic margin off Argentina/Uruguay, South Atlantic, *Mar. Geol.*, *244*(1–4), 46–67, doi:10.1016/j.margeo.2007.06.009.
Funck, T., and H.-U. Schmincke (1998), Growth and destruction of Gran Canaria deduced from seismic reflection and bathymetric data, *J. Geophys. Res.*, *103*, 15,393–15,407, doi:10.1029/98JB00388.
Gaedicke, C., H. Schlüter, H. A. Roeser, A. Prexl, B. Schreckenberger, H. Meyer, C. Reichert, P. Clift, and S. Amjad (2002), Origin of the northern Indus Fan and Murray Ridge, Northern Arabian Sea: Interpretation from seismic and magnetic imaging, *Tectonophysics*, *355*(1–4), 127–143, doi:10.1016/S0040-1951(02)00137-3.
Gaina, C., R. D. Müller, B. Brown, T. Ishihara, and S. Ivanov (2007), Breakup and early seafloor spreading between India and Antarctica, *Geophys. J. Int.*, *170*(1), 151–169, doi:10.1111/j.1365-246X.2007.03450.x.
Gatliff, R. W., K. Hitchen, J. D. Ritchie, and D. K. Smythe (1984), Internal structure of the Erlend Tertiary volcanic complex, north of Shetland, revealed by seismic reflection, *J. Geol. Soc.*, *141*(3), 555–562, doi:10.1144/gsjgs.141.3.0555.
Gernigon, L., J.-C. Ringenbach, S. Planke, and B. Le Gall (2004), Deep structures and breakup along volcanic rifted margins: Insights from integrated studies along the outer Vøring Basin (Norway), *Mar. Pet. Geol.*, *21*(3), 363–372, doi:10.1016/j.marpetgeo.2004.01.005.
Gladczenko, T. P. (1994), Crustal structure and composition of selected transient large igneous provinces, Cand. Sci. thesis, Univ. of Oslo, Oslo.
Gladczenko, T. P., K. Hinz, O. Eldholm, H. Meyer, S. Neben, and J. Skogseid (1997), South Atlantic volcanic margins, *J. Geol. Soc.*, *154*(3), 465–470, doi:10.1144/gsjgs.154.3.0465.
Gladczenko, T. P., J. Skogseid, and O. Eldholm (1998), Namibia volcanic margin, *Mar. Geophys. Res.*, *20*(4), 313–341, doi:10.1023/A:1004746101320.
Gnos, E., A. Immenhauser, and T. Peters (1997), Late Cretaceous/early Tertiary convergence between the Indian and Arabian plates recorded in ophiolites and related sediments, *Tectonophysics*, *271*(1–2), 1–19, doi:10.1016/S0040-1951(96)00249-1.
Gohl, K., and G. Uenzelmann-Neben (2001), The crustal role of the Agulhas Plateau, southwest Indian Ocean: Evidence from seismic profiling, *Geophys. J. Int.*, *144*(3), 632–646, doi:10.1046/j.1365-246x.2001.01368.x.
Gombos, A. M., W. G. Powell, and I. O. Norton (1995), The tectonic evolution of western India and its impact on hydrocarbon occurrences: An overview, *Sediment. Geol.*, *96*(1–2), 119–129, doi:10.1016/0037-0738(94)00129-I.
Hansen, D. M. (2006), The morphology of intrusion-related vent structures and their implications for constraining the timing of intrusive events along the NE Atlantic margin, *J. Geol. Soc.*, *163*(5), 789–800, doi:10.1144/0016-76492004-167.
Hansen, D. M., J. Redfern, F. Federici, D. di Biase, and G. Bertozzi (2008), Miocene igneous activity in the Northern Subbasin, offshore Senegal, NW Africa, *Mar. Pet. Geol.*, *25*(1), 1–15, doi:10.1016/j.marpetgeo.2007.04.007.
Hawkesworth, C., S. Kelley, S. Turner, A. L. E. Roex, and B. Storey (1999), Mantle processes during Gondwana break-up and dispersal, *J. Afr. Earth Sci.*, *28*(1), 239–261, doi:10.1016/S0899-5362(99)00026-3.
Heine, C., R. D. Müller, and C. Gaina (2004), Reconstructing the lost eastern Tethys ocean basin: Convergence history of the SE Asian margin and marine gateways, in *Continent-Ocean Interactions Within East Asian Marginal Seas*, *Geophys. Monogr. Ser.*, vol. 146, edited by P. Clift et al., pp. 37–54, AGU, Washington, D.C.
Hemant, K., and S. Maus (2005), Why no anomaly is visible over most of the continent-ocean boundary in the global crustal magnetic field, *Phys. Earth Planet. Inter.*, *149*(3–4), 321–333, doi:10.1016/j.pepi.2004.10.007.
Henry, S., A. Danfort, and S. Venktraman (2008), Indian continental margin: Diachronous rifting, ridge jumps and continental fragments, paper presented at Rifts Renaissance: Stretching the Crust and Extending Exploration Frontiers, Pet. Group, Soc. for Sediment. Geol., Houston, Tex.
Henstock, T. J., and P. J. Thompson (2004), Self-consistent modeling of crustal thickness at Chagos-Laccadive ridge from bathymetry and gravity data, *Earth Planet. Sci. Lett.*, *224*(3–4), 325–336, doi:10.1016/j.epsl.2004.05.021.
Hirsch, K. K., K. Bauer, and M. Scheck-Wenderoth (2008), Deep structure of the western South African passive margin: Results of a combined approach of seismic, gravity and isostatic investigations, *Tectonophysics*, *470*(1–2), 57–70,doi:10.1016/j.tecto.2008.04.028.
Hopper, J. R., T. Dahl-Jensen, W. S. Holbrook, H. C. Larsen, D. Lizarralde, J. Korenaga, G. M. Kent, and P. B. Kelemen (2003), Structure of the SE Greenland margin from seismic reflection and refraction data: Implications for nascent spreading center subsidence and asymmetric crustal accretion during North Atlantic opening, *J. Geophys. Res.*, *108*(B5), 2269, doi:10.1029/2002JB001996.
Intergovernmental Oceanographic Commission (2003), *Centenary Edition of the GEBCO Digital Atlas* [CD-ROM], Br. Oceanogr. Data Cent., Liverpool, U.K.
Jay, A. E., and M. Widdowson (2008), Stratigraphy, structure and volcanology of the SE Deccan continental flood basalt province: Implications for eruptive extent and volumes, *J. Geol. Soc.*, *165*(1), 177–188, doi:10.1144/0016-76492006-062.

Joppen, M., and R. S. White (1990), The structure and subsidence of Rockall Trough from two-ship seismic experiments, *J. Geophys. Res.*, *95*, 19,821–19,837, doi:10.1029/JB095iB12p19821.

Keen, C. E., and C. Beaumont (1990), Geodynamics of rifted continental margins, in *Geology of the Continental Margin of Eastern Canada*, vol. 2, edited by M. J. Keen and G. L. Williams, pp. 391–472, Geol. Surv. of Can., Ottawa, Ont.

Kent, W., A. D. Saunders, P. D. Kempton, and N. C. Ghose (1997), Rajmahal Basalts, Eastern India: Mantle sources and melt distribution at a volcanic rifted margin, in *Large Igneous Provinces: Continental, Oceanic and Planetary Flood Volcanism*, *Geophys. Monogr. Ser.*, vol. 100, edited by J. J. Mahoney and M. F. Coffin, pp. 145–182, AGU, Washington, D. C.

Kiørboe, L. (1999), Stratigraphic relationships of the Lower Tertiary of the Faeroe Basalt Plateau and the Faeroe-Shetland Basin, in *Petroleum Geology of Northwest Europe: Proceedings of the 5th Conference*, edited by A. Fleet and S. A. R. Boldy, pp. 559–579, Geol. Soc., London.

Komatsu, G., G. G. Ori, P. Ciarcelluti, and Y. D. Litasov (2004), Interior layered deposits of Valles Marineris, Mars: Analogous subice volcanism related to Baikal Rifting, Southern Siberia, *Planet. Space Sci.*, *52*(1–3), 167–187, doi:10.1016/j.pss.2003.08.003.

König, M., and W. Jokat (2010), Advanced insights into magmatism and volcanism of the Mozambique Ridge and Mozambique Basin in the view of new potential field data, *Geophys. J. Int.*, *180*(1), 158–180, doi:10.1111/j.1365-246X.2009.04433.x.

Larsen, H. C., A. D. Saunders, P. D. Clift, and the Shipboard Scientific Party (1994), Breakup of the southeast Greenland margin and the formation of the Irminger Basin: Background and scientific objectives, *Proc. Ocean Drill. Program Initial Rep.*, *152*, 5–16, doi:10.2973/odp.proc.ir.152.101.1994.

Lee, T., and L. A. Lawver (1995), Cenozoic plate reconstruction of Southeast Asia, *Tectonophysics*, *251*(1–4), 85–138, doi:10.1016/0040-1951(95)00023-2.

Lizarralde, D., et al. (2007), Variation in styles of rifting in the Gulf of California, *Nature*, *448*, 466–469, doi:10.1038/nature06035.

Mahoney, J. J. (1988), Deccan Traps, in *Continental Flood Basalts*, edited by J. D. Macdougall, pp. 151–194, Kluwer Acad., Dordrecht, Netherlands.

Mahoney, J. J., C. Nicollet, and C. Dupuy (1991), Madagascar basalts: Tracking oceanic and continental sources, *Earth Planet. Sci. Lett.*, *104*(2–4), 350–363, doi:10.1016/0012-821X(91)90215-4.

Mahoney, J. J., R. A. Duncan, W. Khan, E. Gnos, and G. R. McCormick (2002), Cretaceous volcanic rocks of the South Tethyan suture zone, Pakistan: Implications for the Réunion hotspot and Deccan Traps, *Earth Planet. Sci. Lett.*, *203*(1), 295–310, doi:10.1016/S0012-821X(02)00840-3.

Malod, J. A., L. Droz, B. M. Kemal, and P. Patriat (1997), Early spreading and continental to oceanic basement transition beneath the Indus deep-sea fan: Northeastern Arabian Sea, *Mar. Geol.*, *141*(1–4), 221–235, doi:10.1016/S0025-3227(97)00074-1.

Masson, D. G., T. P. Le Bas, I. Grevemeyer, and W. Weinrebe (2008), Flank collapse and large-scale landsliding in the Cape Verde Islands, off West Africa, *Geochem. Geophys. Geosyst.*, *9*, Q07015, doi:10.1029/2008GC001983.

Maus, S., et al. (2009), EMAG2: A 2-arc min resolution Earth Magnetic Anomaly Grid compiled from satellite, airborne, and marine magnetic measurements, *Geochem. Geophys. Geosyst.*, *10*, Q08005, doi:10.1029/2009GC002471.

Melluso, L., V. Morra, P. Brotzu, L. Franciosi, A. M. Petteruti Lieberknecht, and L. Bennio (2003), Geochemical provinciality in the Cretaceous basaltic magmatism of Northern Madagascar: Mantle source implications, *J. Geol. Soc.*, *160*(3), 477–488, doi:10.1144/0016-764902-060.

Miles, P. R., M. Munschy, and J. Segoufin (1998), Structure and early evolution of the Arabian Sea and East Somali Basin, *Geophys. J. Int.*, *134*(3), 876–888, doi:10.1046/j.1365-246x.1998.00625.x.

Milner, S. C., A. R. Duncan, and A. Ewart (1992), Quartz latite rheoignimbrite flows of the Etendeka Formation, north-western Namibia, *Bull. Volcanol.*, *54*, 200–219.

Minshull, T. A., C. I. Lane, J. S. Collier, and R. B. Whitmarsh (2008), The relationship between rifting and magmatism in the northeastern Arabian Sea, *Nat. Geosci.*, *1*, 463–467, doi:10.1038/ngeo228.

Mitchum, R. M., P. R. Vail, and J. B. Sangree (1977), Stratigraphic interpretation of seismic reflection patterns in depositional sequences, Part 6, in *Seismic Stratigraphy: Application to Hydrocarbon Exploration*, edited by C. E. Payton, 8th ed., pp. 117–133, Am. Assoc. of Pet. Geol., Tulsa, Okla.

Molnar, P., F. Pardo-Casas, and J. Stock (1988), The Cenozoic and Late Cretaceous evolution of the Indian Ocean Basin: Uncertainties in the reconstructed positions of the Indian, African and Antarctic plates, *Basin Res.*, *1*(1), 23–40, doi:10.1111/j.1365-2117.1988.tb00003.x.

Moore, J. G., D. A. Clague, R. T. Holcomb, P. W. Lipman, W. R. Normark, and M. E. Torresan (1989), Prodigious submarine landslides on the Hawaiian Ridge, *J. Geophys. Res.*, *94*, 17,465–17,484, doi:10.1029/JB094iB12p17465.

Moore, J. G., W. R. Normark, and R. T. Holcomb (1994), Giant Hawaiian landslides, *Annu. Rev. Earth Planet. Sci.*, *22*, 119–144, doi:10.1146/annurev.ea.22.050194.001003.

Mountain, G. S., and W. L. Prell (1990), A multiphase plate tectonic history of the southeast continental margin of Oman, in *The Geology and Tectonics of the Oman Region*, edited by A. H. F. Robertson, M. P. Searle, and A. C. Ries, *Geol. Soc. Spec. Publ.*, *49*, 725–743.

Naini, B. R., and M. Talwani (1982), Structural framework and the evolutionary history of the continental margin of western India, in *Studies in Continental Margin Geology*, edited by J. S. Watkins and C. L. Drake, *AAPG Mem.*, *34*, 167–191.

Norton, I. O., and J. G. Sclater (1979), A model for the evolution of the Indian Ocean and the breakup of Gondwanaland, *J. Geophys. Res.*, *84*, 6803–6830, doi:10.1029/JB084iB12p06803.

O'Connor, J. M., P. Stoffers, J. R. Wijbrans, P. M. Shannon, and T. Morrissey (2000), Evidence from episodic seamount volcanism for pulsing of the Iceland plume in the past 70 Myr, *Nature*, *408*, 954–958, doi:10.1038/35050066.

Oh, J., J. A. Austin Jr., J. D. Phillips, M. F. Coffin, and P. L. Stoffa (1995), Seaward-dipping reflectors offshore the southeastern United States: Seismic evidence for extensive volcanism accompanying sequential formation of the Carolina Trough and Blake Plateau Basin, *Geology*, *23*, 9–12, doi:10.1130/0091-7613(1995)023<0009:SDROTS>2.3.CO;2.

Parsiegla, N., K. Gohl, and G. Uenzelmann-Neben (2008), The Agulhas Plateau: Structure and evolution of a Large Igneous Province, *Geophys. J. Int.*, *174*(1), 336–350, doi:10.1111/j.1365-246X.2008.03808.x.

Pawlowski, R. (2008), The use of gravity anomaly data for offshore continental margin demarcation, *Leading Edge*, *27*, 722–727, doi:10.1190/1.2944156.

Peate, D. W., C. J. Hawkesworth, M. S. M. Mantovani, and W. Shukowsky (1990), Mantle plumes and flood-basalt stratigraphy in the Paraná, South America, *Geology*, *18*, 1223–1226, doi:10.1130/0091-7613(1990)018<1223:MPAFBS>2.3.CO;2.

Planke, S., and O. Eldholm (1994), Seismic response and construction of seaward dipping wedges of flood basalts: Vøring volcanic margin, *J. Geophys. Res.*, *99*, 9263–9278, doi:10.1029/94JB00468.

Planke, S., E. Alvestad, and O. Eldholm (1999), Seismic characteristics of basaltic extrusive and intrusive rocks, *Leading Edge*, *18*, 342–348, doi:10.1190/1.1438289.

Planke, S., P. A. Symonds, E. Alvestad, and J. Skogseid (2000), Seismic volcanostratigraphy of large-volume basaltic extrusive complexes on rifted margins, *J. Geophys. Res.*, *105*, 19,335–19,351, doi:10.1029/1999JB900005.

Plummer, P. S., and E. R. Belle (1995), Mesozoic tectono-stratigraphic evolution of the Seychelles microcontinent, *Sediment. Geol.*, *96*(1–2), 73–91, doi:10.1016/0037-0738(94)00127-G.

Presley, T. K., J. M. Sinton, and M. Pringle (1997), Postshield volcanism and catastrophic mass wasting of the Waianae Volcano, Oahu, Hawaii, *Bull. Volcanol.*, *58*, 597–616, doi:10.1007/s004450050165.

Purdy, E. G., and G. T. Bertram (1993), *Carbonate Concepts From the Maldives, Indian Ocean*, *AAPG Stud. Geol.*, 56 pp.

Rabinowitz, P. D., M. F. Coffin, and D. Falvey (1983), The separation of Madagascar and Africa, *Science*, *220*, 67–69, doi:10.1126/science.220.4592.67.

Rey, S. S., S. Planke, P. A. Symonds, and J. I. Faleide (2008), Seismic volcanostratigraphy of the Gascoyne margin, Western Australia, *J. Volcanol. Geotherm. Res.*, *172*(1–2), 112–131, doi:10.1016/j.jvolgeores.2006.11.013.

Robertson, A. H. F., and P. J. Degnan (1993), Sedimentology and tectonic implications of the Lamayuru Complex: Deep-water facies of the Indian passive margin, Indus suture zone, Ladakh Himalaya, in *Himalayan Tectonics*, edited by P. J. Treloar and M. P. Searle, *Geol. Soc. Spec. Publ.*, *74*, 299–321.

Royer, J.-Y., A. K. Chaubey, J. Dyment, G. C. Bhattacharya, K. Srinivas, V. Yatheesh, and T. Ramprasad (2002), Paleogene plate tectonic evolution of the Arabian and Eastern Somali basins, in *The Tectonic and Climatic Evolution of the Arabian Sea Region*, edited by P. D. Clift et al., *Geol. Soc. Spec. Publ.*, *195*, 7–23.

Sandwell, D. T., and W. H. F. Smith (1997), Marine gravity anomaly from Geosat and ERS 1 satellite altimetry, *J. Geophys. Res.*, *102*, 10,039–10,054, doi:10.1029/96JB03223.

Spence, G. D., R. S. White, G. K. Westbrook, and S. R. Fowler (1989), The Hatton Bank continental margin - I. Shallow structure from two-ship

expanding spread seismic profiles, Geophys. *J. Int.*, *96*(2), 273–294, doi:10.1111/j.1365-246X.1989.tb04451.x.

Steinberger, B., and T. H. Torsvik (2008), Absolute plate motions and true polar wander in the absence of hotspot tracks, *Nature*, *452*, 620–623, doi:10.1038/nature06824.

Storey, M., J. J. Mahoney, A. D. Saunders, R. A. Duncan, S. P. Kelley, and M. F. Coffin (1995), Timing of hot spot-related volcanism and the breakup of Madagascar and India, *Science*, *267*, 852–855, doi:10.1126/science.267.5199.852.

Symonds, P. A., S. Planke, O. Frey, and J. Skogseid (1998), Volcanic evolution of the Western Australian continental margin and its implications for basin development, in *The Sedimentary Basins of Western Australia 2*, edited by P. G. Purcell and R. R. Purcell, pp. 33–54, Pet. Explor. Soc. of Aust., Perth, West. Aust.

Thomson, K. (2005), Volcanic features of the North Rockall Trough: Application of visualisation techniques on 3D seismic reflection data, *Bull. Volcanol.*, *67*, 116–128, doi:10.1007/s00445-004-0363-9.

Thomson, K. (2007), Determining magma flow in sills, dykes and laccoliths and their implications for sill emplacement mechanisms, *Bull. Volcanol.*, *70*, 183–201, doi:10.1007/s00445-007-0131-8.

Todal, A., and O. Edholm (1998), Continental margin off western India and Deccan Large Igneous Province, *Mar. Geophys. Res.*, *20*(4), 273–291, doi:10.1023/A:1004640508371.

Torsvik, T. H., R. D. Tucker, L. D. Ashwal, L. M. Carter, B. Jamtveit, K. T. Vidyadharan, and P. Venkataramana (2000), Late Cretaceous India-Madagascar fit and timing of break-up related magmatism, *Terra Nova*, *12*(5), 220–224, doi:10.1046/j.1365-3121.2000.00300.x.

Torsvik, T. H., R. D. Müller, R. Van der Voo, B. Steinberger, and C. Gaina (2008), Global plate motion frames: Toward a unified model, *Rev. Geophys.*, *46*, RG3004, doi:10.1029/2007RG000227.

Vail, P. R., R. G. Todd, and J. B. Sangree (1977), Seismic stratigraphy and global changes of sea level, Part 5: Chronostratigraphy significance of seismic relations, in *Seismic Stratigraphy: Application to Hydrocarbon Exploration*, edited by C. E. Payton, 8th ed., pp. 99–116, Am. Assoc. of Pet. Geol., Tulsa, Okla.

Walker, G. P. L. (1990), Geology and volcanology of the Hawaiian Islands, *Pac. Sci.*, *44*(4), 315–347.

Walker, G. P. L. (1993), Basaltic-volcano systems, in *Magmatic Processes and Plate Tectonics*, edited by H. M. Pritchard et al., *Geol. Soc. Spec. Publ.*, *76*, 3–38.

Wessel, P., and W. H. F. Smith (1995), New version of the generic mapping tools released, *Eos Trans. AGU*, *76*(33), 329, doi:10.1029/95EO00198.

White, R. S. (1992), Magmatism during and after continental break-up, in *Magmatism and the Causes of Continental Break-up*, edited by T. Alabaster and R. J. Pankhurst, *Geol. Soc. Spec. Publ.*, *68*, 1–16.

White, R. S., and K. E. Louden (1982), The Makran continental margin: Structure of a thickly sedimented convergent plate boundary, in *Studies in Continental Margin Geology*, edited by J. S. Watkins and C. L. Drake, *AAPG Mem.*, *34*, 499–518.

White, S. M., J. A. Crisp, and F. J. Spera (2006), Long-term volumetric eruption rates and magma budgets, *Geochem. Geophys. Geosyst.*, *7*, Q03010, doi:10.1029/2005GC001002.

Wood, M. V., J. Hall, and J. J. Doody (1988), Distribution of early Tertiary lavas in the NE Rockall Trough, in *Early Tertiary Volcanism and the Opening of the NE Atlantic*, edited by A. C. Morton and L. M. Parson, *Geol. Soc. Spec. Publ.*, *39*, 283–292.

Yatheesh, V., G. C. Bhattacharya, and J. Dyment (2009), Early oceanic opening off Western India-Pakistan margin: The Gop Basin revisited, *Earth Planet. Sci. Lett.*, *284*(3–4), 399–408, doi:10.1016/j.epsl.2009.04.044.

G. Calvès, LMTG, Université de Toulouse Paul Sabatier, SVT-OMP, 14 ave. Edouard Belin, F-31400 Toulouse, France. (gerome.calves@lmtg.obs-mip.fr)

P. D. Clift and D. Jolley, Department of Geology and Petroleum Geology, School of Geosciences, University of Aberdeen, Meston Building, Aberdeen, AB24 3UE, UK.

C. Gaina, Geological Survey of Norway, NO-7491 Trondheim, Norway.

M. Huuse, School of Earth, Atmospheric, and Environmental Sciences, University of Manchester, Williamson Building, Oxford Road, Manchester, M13 9PL, UK.

A. Inam and A. R. Tabrez, National Institute for Oceanography, ST-47-Block 1, Clifton, Karachi 75600, Pakistan.

A. M. Schwab, Marathon International Petroleum (GB), Ltd., Marathon House, Rubislaw Hill, Anderson Drive, Aberdeen AB15 6FZ, UK.